

UNCLASSIFIED

AD NUMBER
ADB282119
NEW LIMITATION CHANGE
TO Approved for public release, distribution unlimited
FROM Distribution authorized to U.S. Gov't. agencies only; Proprietary Information; Sep 2001. Other requests shall be referred to US Army Medical Research and Materiel Command, 504 Scott Street, Fort Detrick, MD 21702
AUTHORITY
USAMRMC ltr, 21 Feb 2003

THIS PAGE IS UNCLASSIFIED

AD \_\_\_\_\_

Award Number: DAMD17-98-1-8177

TITLE: Visual Servicing for Optimization of Anticancer Drug Uptake in Human Breast Cancer

PRINCIPAL INVESTIGATOR: Daniel E. Callahan, Ph.D.

CONTRACTING ORGANIZATION: University of California at Berkeley  
Berkeley, California 94720

REPORT DATE: September 2001

TYPE OF REPORT: Final

PREPARED FOR: U.S. Army Medical Research and Materiel Command  
Fort Detrick, Maryland 21702-5012

DISTRIBUTION STATEMENT: Distribution authorized to U.S. Government agencies only (proprietary information, Sep 01). Other requests for this document shall be referred to U.S. Army Medical Research and Materiel Command, 504 Scott Street, Fort Detrick, Maryland 21702-5012.

The views, opinions and/or findings contained in this report are those of the author(s) and should not be construed as an official Department of the Army position, policy or decision unless so designated by other documentation.

20020909 065

## NOTICE

USING GOVERNMENT DRAWINGS, SPECIFICATIONS, OR OTHER DATA INCLUDED IN THIS DOCUMENT FOR ANY PURPOSE OTHER THAN GOVERNMENT PROCUREMENT DOES NOT IN ANY WAY OBLIGATE THE U.S. GOVERNMENT. THE FACT THAT THE GOVERNMENT FORMULATED OR SUPPLIED THE DRAWINGS, SPECIFICATIONS, OR OTHER DATA DOES NOT LICENSE THE HOLDER OR ANY OTHER PERSON OR CORPORATION; OR CONVEY ANY RIGHTS OR PERMISSION TO MANUFACTURE, USE, OR SELL ANY PATENTED INVENTION THAT MAY RELATE TO THEM.

### LIMITED RIGHTS LEGEND

Award Number: DAMD17-98-1-8177

Organization: University of California at Berkeley

Those portions of the technical data contained in this report marked as limited rights data shall not, without the written permission of the above contractor, be (a) released or disclosed outside the government, (b) used by the Government for manufacture or, in the case of computer software documentation, for preparing the same or similar computer software, or (c) used by a party other than the Government, except that the Government may release or disclose technical data to persons outside the Government, or permit the use of technical data by such persons, if (i) such release, disclosure, or use is necessary for emergency repair or overhaul or (ii) is a release or disclosure of technical data (other than detailed manufacturing or process data) to, or use of such data by, a foreign government that is in the interest of the Government and is required for evaluational or informational purposes, provided in either case that such release, disclosure or use is made subject to a prohibition that the person to whom the data is released or disclosed may not further use, release or disclose such data, and the contractor or subcontractor or subcontractor asserting the restriction is notified of such release, disclosure or use. This legend, together with the indications of the portions of this data which are subject to such limitations, shall be included on any reproduction hereof which includes any part of the portions subject to such limitations.

THIS TECHNICAL REPORT HAS BEEN REVIEWED AND IS APPROVED FOR PUBLICATION.

  
\_\_\_\_\_

  
\_\_\_\_\_

# REPORT DOCUMENTATION PAGE

Form Approved  
OMB No. 074-0188

Public reporting burden for this collection of information is estimated to average 1 hour per response, including the time for reviewing instructions, searching existing data sources, gathering and maintaining the data needed, and completing and reviewing this collection of information. Send comments regarding this burden estimate or any other aspect of this collection of information, including suggestions for reducing this burden to Washington Headquarters Services, Directorate for Information Operations and Reports, 1215 Jefferson Davis Highway, Suite 1204, Arlington, VA 22202-4302, and to the Office of Management and Budget, Paperwork Reduction Project (0704-0188), Washington, DC 20503

<b>1. AGENCY USE ONLY (Leave blank)</b>		<b>2. REPORT DATE</b> September 2001	<b>3. REPORT TYPE AND DATES COVERED</b> Final (1 Sep 98 - 31 Aug 01)	
<b>4. TITLE AND SUBTITLE</b> Visual Servicing for Optimization of Anticancer Drug Uptake in Human Breast Cancer			<b>5. FUNDING NUMBERS</b> DAMD17-98-1-8177	
<b>6. AUTHOR(S)</b> Daniel E. Callahan, Ph.D.				
<b>7. PERFORMING ORGANIZATION NAME(S) AND ADDRESS(ES)</b>  University of California at Berkeley Berkeley, California 94720  <b>E-mail:</b> <a href="mailto:DECallahan@lbl.gov">DECallahan@lbl.gov</a>			<b>8. PERFORMING ORGANIZATION REPORT NUMBER</b>	
<b>9. SPONSORING / MONITORING AGENCY NAME(S) AND ADDRESS(ES)</b>  U.S. Army Medical Research and Materiel Command Fort Detrick, Maryland 21702-5012			<b>10. SPONSORING / MONITORING AGENCY REPORT NUMBER</b>	
<b>11. SUPPLEMENTARY NOTES</b> Report contains color				
<b>12a. DISTRIBUTION / AVAILABILITY STATEMENT</b> Distribution authorized to U.S. Government agencies only (proprietary information, Sep 01). Other requests for this document shall be referred to U.S. Army Medical Research and Materiel Command, 504 Scott Street, Fort Detrick, Maryland 21702-5012.				<b>12b. DISTRIBUTION CODE</b>
<b>13. ABSTRACT (Maximum 200 Words) PURPOSE:</b> Develop an instrument (a visual-servoing optical microscope, or VSOM) and gather preliminary data that demonstrate the capabilities of this instrument. <b>SCOPE:</b> A VSOM was constructed, and VSOM assay feasibility was demonstrated. A clinically tested calcein assay for Multi-Drug Resistance (MDR) was used to demonstrate the advantages of VSOM assays. <b>RESULTS:</b> Relevant perturbations and stimulations were successfully applied via computer-controlled perfusion pumps during VSOM assays. Dynamic physiological responses of single human breast tumor cells (300-800 cells) were analyzed in multiple channels for 1-5 h. The characteristics of individual cells were quantified, resulting in a unique "physiological fingerprint" for each cell. Preliminary data for VSOM apoptosis and proliferation assays were also obtained, and new algorithms for cell segmentation were developed. New funding was obtained through the U.S. Department of Energy, a U.S. patent application was filed, and presentations were made at national scientific meetings. In addition, the LBNL Technology Transfer Office is entering into a licensing agreement with an outside company that will facilitate commercial VSOM development. <b>SIGNIFICANCE:</b> VSOM methods and devices will be useful for executing MDR fluorescence assays, developing additional assays, and developing optimized microenvironments for improved ex vivo propagation and drug response testing of human breast tumor biopsies.				
<b>14. SUBJECT TERMS</b> Breast Cancer, multidrug resistance, fluorescence microscopy, calcein				<b>15. NUMBER OF PAGES</b> 57
				<b>16. PRICE CODE</b>
<b>17. SECURITY CLASSIFICATION OF REPORT</b> Unclassified	<b>18. SECURITY CLASSIFICATION OF THIS PAGE</b> Unclassified	<b>19. SECURITY CLASSIFICATION OF ABSTRACT</b> Unclassified	<b>20. LIMITATION OF ABSTRACT</b> Unlimited	

## Table of Contents

<u>Section</u>	<u>Page</u>
Cover.....	
SF 298.....	2
Table of Contents.....	3
Introduction.....	4
Body.....	4-15
Key Research Accomplishments.....	16
Reportable Outcomes.....	17
Conclusions.....	18-19
References.....	20-21
Appendix A: Figures with Legends.....	22-28
Appendix B: Abstract, 2002 Annual Meeting Biophysical Society.....	29-30
Appendix C: Two Abstracts for two 2002 AACR Meetings.....	31-33
Appendix D: U.S. Patent Application, VSOM Methods and Devices.....	34
Appendix E: Poster & Abstract, 2001 Biophysical Society Annual Meeting.....	35-49
Appendix F: LBNL Software Disclosure Form.....	50
Appendix G: Grant Proposal, to NSF/NIGSM .....	51
Appendix H: Grant Proposal, to CA BCRP Cycle 7.....	52
Appendix I: Patent Disclosure IB-1559P1, VSOM Control Software .....	53
Appendix J: Publications resulting from this research.....	54
Appendix K: Personnel receiving pay from this research.....	55
Appendix L: ABBREVIATIONS & ACRONYMS.....	56

## Introduction

Recent clinical studies of acute myeloid leukemia (AML) patients have demonstrated the important predictive and prognostic capabilities of the calcein *in vitro* assay for multidrug resistance (MDR) [1, 2]. These studies employed the fluorescent compound calcein, various MDR reversal agents, and flow cytometry in functional assays for the MDR proteins P-glycoprotein (Pgp) and multidrug resistance-associated protein (MRP). The assays, performed on fresh leukemia cells, required 4-6 hrs to complete and were prognostic for complete remission (CR), therapy failure, and survival rate. **The ultimate goal(s) of our research are to (i) develop an instrument, software, and bioinformatics infrastructure that will allow us to (ii) develop improved *ex vivo* fluorescence assays such as assays for microenvironment design, drug response and multidrug resistance, and (iii) improve primary tumor cell culture microenvironments so that tumor cells freshly derived from the solid tumors of individual breast cancer patients can be successfully propagated and tested *ex vivo*.** The immediate objective of our research was to develop and demonstrate the capabilities of a visual servoing optical microscope (VSOM) that would allow prolonged real-time interactive manipulations and observations on living breast cancer cells. Visual servoing (VS) is a term from the field of robotic vision; it refers to the dynamic manipulation of experimental parameters based on analysis of digital image content. In VSOM assays, the flow rates of computer-controlled syringes are adjusted based on the detection and quantification of single-cell physiological responses. In such assays, cells are attached to a surface in a microincubation chamber as various solutions are perfused through the chamber. On-line detection (digital image segmentation) of individual cells, intelligent control of syringes, and on-going analysis of single cell responses is required for VSOM experiments. Unlike flow cytometry, VS microscopy monitors and repeatedly stimulates living cells for an extended period of time. In the future, adaptive, responsive, and intelligent control of applied perturbations and stimuli will benefit greatly from real-time access to an on-line database of previously observed cell responses and biological outcomes. We believe the VSOM approach represents a new paradigm for *in vitro* drug response and chemosensitivity testing, and we demonstrate herein preliminary data that demonstrate the advantages and feasibility of our approach.

## Body

The purpose of this 2-year IDEA proposal was to gather preliminary data that demonstrate the feasibility and advantages of visual servoing optical microscope (**VSOM**) technology, software, and assays. The 3-year IDEA project that was originally proposed was cut to 2 years, and funding was reduced 33% (from \$358,796 to \$238,872). This final year (Year 3, 2000-2001) is a no-cost extension provided at no additional charge. It should be noted that extensive additional financial support for the experiments, instrumentation, salary, software and bioinformatics infrastructure that supported this research was provided by several other on-going, funded research projects. Thus, we successfully leveraged other funding to provide support for this VSOM research, and we also obtained additional funding from other sources to continue this VSOM research. This is our Final Report ("FP"). Additional references and details can be found in the original proposal ("OP", June 1997), the approved revisions to the original proposal ("AROP", July 1998), the Year 1 Annual Report ("AR#1", October 1999), and the Year 2 Annual Report ("AR#2", October 2000). As stated in the AROP, *"Our objectives are to develop the VSOM in a stepwise fashion and gather preliminary data to aid future development of cell culture techniques and fluorescence assays."*

In this IDEA grant, assays for one important type of multidrug resistance (MDR) were targeted, that of enhanced efflux and decreased influx of anticancer drugs[3]. A related mechanism, increased drug sequestration within tumor cells, was also briefly examined[4]. However, as noted in AR#1 (1998-1999: page 7 and Figure 9), one of the VSOM assays we initially proposed (Task 7b, detection of acidification defects using LT-Red and monesin) was found to be unsuitable for VSOM instrument development, especially when used with the MCF-7 cells obtained from our colleague, Dr. R. Lupu. For this reason, we obtained a new set of matched cells (MCF-7 WTC and MCF-7 ADR cells from Dr. A. Parissenti) and focused solely on the second assay we proposed to study (Task 7a, detection of Pgp and MRP using calcein-AM and verapamil). For this reason, no further experiments were performed using the LT-Red assay(s) as proposed in Task 7b. *The changes to this task did not*

involve changes in (i) methodology, (ii) stated objectives, or (iii) phenomena under study. Thus, prior approval was not obtained prior to making these changes.

Our increased focus on calcein assays (the influx/efflux MDR mechanism) was also based on important clinical results that were published after the approval of our revised research objectives[1, 2, 5]. Clinical studies have demonstrated that a calcein assay successfully predicts both (i) positive responses to chemotherapy (72% predictive value), (ii) therapy failure (69% predictive value), and survival rate for AML patients[1]. In addition, calcein assays have been shown to be prognostic for achievement of CR in AML patients. Although it has yet to be proven that the presence of Pgp and MRP contribute to treatment failure in breast cancer, important *in vitro* drug response assays (on 359 freshly resected specimens of breast carcinoma) strongly imply that Pgp expression by breast carcinoma is a clinically relevant mechanism of drug resistance for drugs such as doxorubicin and paclitaxel [5]. Data presented in this study strongly suggest that (i) the degree of Pgp expression may significantly contribute to the level of clinical resistance to paclitaxel and doxorubicin, and (ii) prior therapy with chemotherapeutic agents that are substrates for Pgp may induce Pgp expression and select for Pgp-overexpressing tumor cells at relapse[5].

Calcein is an intensely fluorescent, relatively nontoxic surrogate compound for certain anticancer drugs, and this allows one to test for the specific influx/efflux defenses present in living breast tumor cells[1, 2]. When used in conjunction with MDR modulators such as verapamil, cyclosporin A, PSC-833, benzbromarone, or MK-571, the fluorescent probe CAL and other fluorescent probes can be used to obtain detailed information about the amount and types of efflux defenses present in any given cell[6-9]. We participated in the  $\beta$ -testing of an MDR assay which is now clinically tested and commercially available ("MultiDrugQuant Assay Kit" for haematological tumors, Solvo Biotechnology, Budapest, Hungary, [www.solvo.hue](http://www.solvo.hue)). In order to participate in the  $\beta$ -testing of this kit we needed to include a second compound (MK-571) to our VSOM assays. The addition of MK-571 to our VSOM calcein assays resulted in remarkable "physiological fingerprints" (discussed below) that not only differentiate between MDR and DS cells, but also clearly demonstrated the previously reported loss of the MDR phenotype as a function of time spent in cell culture[10]. The development of these important results required the development of high passage number (PN) MCF-7 WTC and MCF-7 ADR cells (Parissenti WTC and ADR cells, PN=27, and PN=23, respectively) representing a time in culture of 24 weeks. (see **Appendix C**, 2002 AACR abstract entitled, "A VSOM calcein assay for quantitation of multidrug resistance in human breast cancer cells", to be presented at the 93rd Annual Meeting of the AACR, San Francisco, April 6-10, 2002, Abstract ID 106867).

In addition, we have demonstrated that our VSOM technology, when coupled with the bioinformatics capabilities developed in our other research projects (*DeepView* and *BioSig*), has unique capabilities that will allow for the rapid, automated, and intelligent extraction of MDR phenotypic data from large numbers of individual, living, human breast cancer cells (**Appendix B**, Biophysical Society Abstract). This abstract has been scheduled in a Platform Session at the 46th Biophysical Society Annual Meeting in San Francisco, California, February 23-27, 2002, and is entitled "BioSig: A Database for Efficient VSOM Extraction of Dynamic Phenotypic Data from Individual Living Cells" (Platform S - Biophysical Chemistry & Emerging Techniques, Monday, February 25, 2002, Program #860-Plat).

Many of our important accomplishments do not appear in the "Technical Objectives and Tasks" list below. For example, submission of a patent application, licensing of our technology to an outside company, and integration of our VSOM system with an advanced, remote bioinformatics system were accomplished, but do not fall into any of the original tasks or objectives. As discussed in our follow-up grant proposal to this research (AR#2, Appendix G, pgs 76-95; not funded) we demonstrated our ability to integrate Cancer Biologists into our effort, in a way that would have directly addressed problems with primary breast cancer and metastatic cell culture techniques. In this proposal, we also addressed the basic limitations of cell-line *in vitro* chemosensitivity and predictive assays, and we proposed a detailed 3-year strategy for bringing this technology into clinical trials. Although DoD BCRP declined to fund the continuation of this research, we used our preliminary data to obtain new multi-year funding from the Office of Biological and Environmental Research (**OBER**) in the Office of Science (OS), U.S. Department of Energy (DOE) (currently in Year 2 of funding, see AR#2 for a copy of this proposal in Appendix G, pgs 120-151).

**Current Funding:** In our current OBER project, we will use VSOM to design new fluorescent analogs of antisense compounds[11-14] that will allow quantitative imaging of gene expression (i.e., mRNA levels of specific genes). Our initial target is the BCL-2 gene, and we are attempting to image the levels of mRNA transcribed from this gene. The Bcl-2 protein is used as a defense against the cellular apoptosis (programmed cell death) induced by anticancer agents[15-24]. Alterations in apoptosis (such as overexpression of bcl-2) are considered an independent mechanism of multidrug resistance[3]. The anti-Bcl-2 antisense compound we are modifying is "G3139"[25-30]. We will make a presentation of our preliminary results in a poster entitled, "Bcl-2 mRNA as a Target for Antisense Imaging Agents: Digital Imaging Fluorescence Microscope Studies of F-G3139, a Fluorescently-labeled Phosphorothioate." Callahan, D.E., Parvin, B.<sup>1</sup>, and Taylor, S.E. at "*Molecular Imaging in Cancer: Linking Biology, Function, and Clinical Applications In Vivo*", an AACR Special Conference in Cancer Research, January 23-27, 2002, Lake Buena Vista, FL. Thus, we are continuing to develop VSOM technology and fluorescence assays in our current work. The ability to image the expression of specific genes in living cells, and the changes in gene expression induced by specific microenvironments and perturbations will help us achieve our ultimate goals of **(i) developing new *ex vivo* fluorescence assays for microenvironment design, drug response and multidrug resistance, and (ii) improving primary tumor cell culture microenvironments so that tumor cells freshly derived from the solid tumors of individual breast cancer patients can be successfully propagated and tested *ex vivo*.**

The detailed description of our Technical Objectives and Tasks is presented below.

**Technical Objective 1:** *Automated design of an optimized protocol for overcoming multidrug resistance in a mixed population of DS and MDR human breast cancer cells.*

**Task 1:** Develop a graphical user interface (GUI) for a prototype, non-automated VSOM system.

**COMPLETED WITH CHANGES.** *The changes to this task did not involve changes in (i) methodology, (ii) stated objectives, or (iii) phenomena under study. Thus, prior approval was not obtained prior to making these changes.*

A new platform-independent VSOM GUI was developed this year. This GUI, which is a JAVA program called "MainFrame", constructs command files for underlying software derived from the VX5 and ADR software discussed in AR#2 (page 6). The LBNL software disclosure form for this collection of software, called "VSOM1", is included in Appendix F. As seen in Figure 1 (Appendix A), this VSOM GUI is composed of three tabbed sections called "Pump Scheduler", "Scope Scheduler", and "I/O". The user begins on the Pump Scheduler tabbed page by specifying how many Pump Intervals the VSOM experiment will have. Collections of Pump Intervals (or cell "Exposures") are sometimes referred to as "Recipes". Examples of pump intervals were shown and discussed in AR#2 (page 11 and Figure 9). To summarize, the user specifies distinct time intervals and then specifies the syringe pump that will operate during each time interval, the rate at which it will operate, and the duration of pump activity. Several fields allow the user to specify fluorescence intensity threshold conditions that can override user-specified perfusion times. For example, if an upper threshold of mean cellular fluorescence intensity is reached in 5 minutes, rather than in the 30 minutes initially specified, the system will stop the current pump and move on to the next perfusion interval. If the threshold is never reached, then pump operation will terminate at the specified 30 minute time point. Automation and documentation features such as these allow for the automated design of compound exposure, incubation, and washout/rinsing protocols. Fields for annotation of syringe contents and other experimental parameters are also provided. The second tabbed page, "Scope Scheduler", allows additional experimental annotation and also allows the user to specify the number of image channels, the wavelength of each image channel, the exposure time for each image channel, the time intervals for digital image acquisition, and the maximum allowed duration of the entire experiment. Two methods of dark current digital image correction can also be specified: (i) acquire a dark current image once at the outset of the experiment, or (ii) acquire a dark current image every time a specimen image is acquired. The last tabbed page, "I/O" allows additional experimental annotation and indicates where the digital images are to be stored.

**Technical issues:**

Our current prototype VSOM system is shown in Figure 2 (Appendix A). As seen in this figure, a Sun Ultra2 workstation ("A") communicates with upper port ("D2") and lower port ("D1") digital cameras via S-Bus SDV interface boards contained within the computer. This Zeiss Axiovert 135 inverted microscope ("C") also has a standard 35mm camera ("D3") for standard color photographs. Two dual-syringe, computer controlled perfusion pumps ("E1,2") are located near the microscope and communicate with the computer via daisy-chaining of RS-232 cables. Other microscope peripherals such as the rotating optical filter wheel, the transmitted and epifluorescence shutters, the scanning xy stage and the z-axis stepper motor (for focusing) are computer-controlled via a Ludl control unit ("B") which accepts commands from the host computer ("A"). Thus, we are currently limited to a total of (4) 60cc syringes per automated experiment. It should be noted that other funds from other sources were used to purchase the second dual-syringe perfusion pump. In non-automated experiments, however, the user may replace, swap, or refill syringes during the course of an experiment. Several non-computer controlled temperature regulation units ("F1,2", Harvard Instruments Models TC-202 and TC-202A) are used with various microperfusion chambers to maintain a chamber temperature of 37° C. The entire system can be operated remotely via standard 100BaseT Ethernet connections ("G"). Both of our microperfusion chambers (discussed below) can be mated with copper tubing to allow for additional heating or cooling via a circulating water bath ("H"). Excess liquid is aspirated from the chamber using a vacuum pump ("I") and a dual

Erlenmeyer flask trap for aspirated liquid ("J"). The maximum perfusion rate using this vacuum system is approximately 5 mL/min.

Several important technical issues regarding the design and use of temperature-controlled microperfusion cell chambers arose during proof-of-principle VSOM experiments. Our previous model was a Harvard PDMI-2 for 35mm cell culture dishes (AR#2 Figure 6G, page 31; also "A", page 46). These open dishes did not fit snugly into the chamber and a small, variable amount of motion occurred during VSOM experiments. In addition, it was difficult to maintain a temperature of 37° C at perfusion flow rates below 0.5 mL/min, and the relatively thick plastic bottom of the dish (i) prevented us from using higher resolution oil-immersion objectives (which require cells attached to a 0.17mm thick coverslip/coverglass) and (ii) attenuated fluorescence excitation and emission light, especially below 360nm. The latter item made 340/380nm calcium ratio imaging studies difficult. Harvard Instruments does provide teflon-coated glass coverslip dishes to address these issues, but these dishes have a severe leakage problem and are not reliable. Several different O-rings were used to seal these chambers, however, we continued to experience leakage problems and cytotoxicity issues. For this reason, we moved to a different type specimen vessel, referred to as a "chambered coverglass" vessel (**Figure 3A**). These vessels are commercially available in sterile packages (through Nunc/LabTek) and are available with 1,2,4, or 8 individual chambers. Thus, the chamber volume can be made very small by choosing smaller chamber coverglass vessels. Using funds from other funding sources, we purchased and modified a new microperfusion chamber from Harvard Instruments (**model CSMI**, Figure 3B). As seen in Figure 3C, the aspirator (red arrow) and temperature probe (blue arrow) must be inserted into the coverglass chamber; thus, we currently perform VSOM experiments in 1 or 2 chamber coverglass vessels only. Our computer-controlled scanning stage required extensive modifications in order to fit the early PDMI-2 microperfusion chamber (AR#2, Figure 6D, page 31). For this reason, we have begun to use stage plate inserts (AR#2, Figure 6E,F, page 31) that can hold various sizes and numbers of specimen vessels. The new CSMI microperfusion chamber was mated to such an aluminum stage plate insert (Figure 3B, green arrow) so that it would fit not only into a computer-controlled scanning stage, but also into a Zeiss standard mechanical stage (Figure 6C). We required a separate microscope stage (non-computer-controlled) in order to isolate the cause of specimen vessel motion during VSOM experiments. This mechanical stage was obtained using funds from other funding sources. In addition, we obtained a Nevtek Air Stream Incubator (model ASI-400, Figure 3D) using funds from other funding sources. The ASI-400 was positioned underneath the CSMI and warm air was directed at the bottom of the chambered coverglass vessel, as shown in Figure 3D. This additional heating source assisted the Harvard TC-202A temperature regulation unit and resulted in greater temperature stability. This allowed us to perform longer-term VSOM experiments using much slower perfusion flow rates (0.1mL/min), even when limited to a total syringe capacity of 240mL (i.e., four 60mL syringes). In addition, it was also easier to alternate between slower flow rates (or no flow) and faster flow rates during consecutive perfusion intervals. One important technical issue is the fact that Harvard microperfusion chambers preheat perfusion liquid in the body of the chamber before delivering it to the specimen vessel. If the flow rate varies, the amount of preheating varies since the perfusion liquid spends a variable amount of time in the preheating area of the microperfusion chamber. This results in unacceptable temperature variations in the specimen vessel (as measured by the specimen chamber temperature probe shown in Figure 3C), unless the Air Stream Incubator is employed. We believe our earlier specimen motion problem was a direct result of variations in temperature, and we no longer experience this problem using the experimental setup shown in Figure 3.

**Task 2:** Optimize algorithms for detecting individual cells in transmitted light by analyzing image data off-line.

**COMPLETED.** This task was completed and discussed extensively in AR#2, pp. 7-9, and Figure 5.

**Task 3:** Display, then allow operator to control the perfusion of an agent(s) and display cellular responses visually (display image channels) and graphically (mean cellular fluorescence for all cells) on the computer screen in real-time, during the experiment.

**COMPLETED WITH CHANGES.** *The changes to this task did not involve changes in (i) methodology, (ii) stated objectives, or (iii) phenomena under study. Thus, prior approval was not obtained prior to making these changes.*

The ADR software discussed in AR#2 (page 6 and Figure 9 and lower half of Figure 9) displays the mean population cell responses on-screen during VSOM experiments. The **MainFrame GUI** (see Task 1, above) is used to control the perfusion of various agents. The MainFrame GUI also allows the user to display two image windows in the computer monitor during an experiment (See Figure 1, "Scope Scheduler | Display Channel"). One image window always displays the transmitted light image, because cells are always visible in this channel, even when they do not contain fluorescent dyes. The user then selects the fluorescence channel to be displayed in the second image window. For example, the green fluorescence channel is often chosen as the Display Channel during calcein retention experiments, because the user can see (by referring back to the transmitted light channel) what percent of the cells are retaining calcein, and to what degree. The heterogeneity of the population response is also seen.

A human operator did not control the perfusion of agents because the the cell responses that were displayed on the screen "in real-time" were very slow on a human time scale. Human operators could not sit in front of the computer screen and get any real sense of what is happening in the experiment, because (i) the cell responses we observed were slow and took place over many hours, and (ii) the mean response curve of many hundreds of cells plotted on the computer screen was not found to be informative. For this reason, we developed several novel ways of plotting and reviewing cellular responses. Human operators interacted with data sets that had been automatically processed, and carefully verified the accuracy of the automatic analyses and indentified technical problems. One useful graphical visualization method was shown in AR#2, Figures 12, 16, and 17. These are 3D "ribbon" cellular response curves, and are very useful for visualization of individual dynamic cellular responses across multiple channels. In addition, time-lapse video sequences can be constructed and "speeded-up" so that a human operator can review them on a "human" time-scale. As discussed in AR#2 (Task 1, page 5 and Figure 2), these data review sessions are intimately connected to the separate, remote DeepView/BioSig bioinformatics system (located approximately 1 mile away in the Building 50 laboratories of Dr. Parvin, and funded via a separate funding mechanism) via the Java VSOM Results Browser. Copious annotation of experiments is accomplished via both real-time annotation of instrument parameters (AR#2, Figure 3) and manual post-experiment annotation via the Java Command File Generator (JCFG) (AR#2, Figure 1). This allows automated construction and annotation of time-lapse movies using variously colored cell outlines constructed from stored cell coordinates and number labels, cell contour (outline) coordinates, pump logs, time stamps, and other stored experimental annotation files.

Additional human operator interaction with, and visualization of, experimental data was accomplished on local computers using automated software that resides locally. The Scil Image Software package (TNO Institute of Applied Physics, Delft, The Netherlands) and custom-written C programs are used on both SUN Unix computers and MS Windows PC computers. Custom versions of Scil Image are compiled (separately on each platform) that contain custom-written C language programs. These programs use command files generated by the JCFG which aggregates data from various annotation files. For example, these programs include `parse_ucf.c`, `ucf_process.c`, `ucf_tiff.c`, and `track_motion.c`. It should be noted that the PC-based Scil Image software package and the Microsoft Visual Studio required for program compilations

**parse\_ucf.c:** This program parses the command file generated by the JCFG and reassembles the information in various useful text files which serve as input for other programs.

**ucf\_process.c:** This program displays all the raw experimental image data from all channels and circles the pixels of maximum intensity, so that a user can visually determine whether or not the image intensity maxima found throughout the image set are valid for image scaling from 0-4094 (the intensity scale of our 12-bit camera) to 0-255 (the 8-bit intensity scale that can be displayed on a computer monitor). Often bright fluorescent specks are found which are not true signal. Thus, the user must choose an alternative maximum intensity for scaling and subsequent image presentation. This becomes very important when generating digital video or color composite images for presentation. Subsequently, the user's choices of minimum and maximum intensities are recorded in an annotation file. In addition, this program calculates an image background intensity value and an image signal intensity threshold value by fitting a parabola to the major (background intensities) peak in the image intensity histogram. The peak of the (inverted) parabola is taken to be the modal value of the background peak, and an

extrapolation is made to a fluorescence signal threshold value (of higher intensity than the background peak) using the formula for the parabola that was fitted to the background intensity peak in the intensity histogram.

**ucf\_tiff.c:** This program scales 12-bit images (0-4095 intensity scale) to 8-bit (0-255 intensity scale) and places images in the appropriate artificially colored image channel. 16-bit tiff images (used by some PC-based image analysis software packages such as Sigma Scan Pro) can also be generated. The user can examine the resultant set of images (often more than 100 images per channel) and rescale the entire set, if necessary.

**track\_motion.c:** This program places a colored outline, and a number label on each cell and allows the user to step through the image set on a frame-by-frame basis. These colored outlines ("contours") can be placed in any displayed image channel, so that one can see how contours derived from the blue nuclear fluorescence channel (AR#2, page 49 "B") map onto other image channels such as the transmitted light channel (AR#2, page 49, "A"), or the green fluorescence image channel (AR#2, page 50 "B"), or the red fluorescence image channel (AR#2, page 51 "B"), or a color composite image (AR#2, page 52 "A" and "B"). An example of cell contours overlaid on a fluorescence images were shown in AR#2 (page 53, "E" and page 56 "E") and are also shown in **Appendix E** (cell nucleus contours, Figures 6A,B).

Human operators "stepped through" many image sets in order to verify the accuracy of cell number labeling, cell tracking, and cell outlining. This process was combined with visual analysis of the 3D ribbon plots of cellular responses. Using this method, it was possible to identify any technical issues that led to spurious single cell responses in our 3D graphs. These spurious single cell responses (individual ribbon plots) could be isolated from the other (many hundreds) cell responses, and the misassignments could be analyzed. This ultimately improved individual cell tracking through long or discontinuous VSOM experiments. The ability to compare very weak cellular fluorescence signals to the visible cells seen in the transmitted light channel was invaluable for improving our cell detection and tracking software.

**vsingle.c:** This program was used to detect cell and generate image contours (outlines) that were used in programs that required contours.

**sorted\_ribbons.c:** This program was used off-line by a human operator to correct and further characterize technical issues identified with the "track\_motion.c" software (above). The main technical problem encountered during long (or discontinuous: see Biophysical Society Poster, 2001, **Appendix E**, Figure 7 and AR#2 Experiment WA4, p.14) VSOM experiments was the fact that image processing algorithms such as "vsingle.c" (discussed above) sometimes detected a variable number of cells from frame to frame. This can cause cell number labels to vary from frame to frame causing discontinuities in individual ribbon plots as a particular cell number label is moved from cell to cell. Cells can move or disappear in VSOM experiments, and the microscope stage, microperfusion chamber or specimen vessel can move between time points. Thus, cell contours must be recalculated for each image of a time series, and the cells have to be tracked from frame to frame, matched properly, and then resorted to match the original (first time-point) cell number labeling. This must be done before generating graphs or annotated video of time-dependent cell responses. The program sorted\_ribbons uses the calculated center of mass (CM) X coordinate, the CM Y coordinate, and the shape of the nucleus to identify and track each cell from frame to frame. A report is given at the end of this sorting/tracking/matching procedure. The percentage of successful frame to frame cell matches is reported as a percent of the starting number of detected cells (or the percentage of cells that could be followed all the way through the experiment).

**Task 4:** Use mixed population of cells and indicate cell type with a specific color outline. Allow operator to observe at what point the system makes a decision identifying cell type and display plots of mean cellular fluorescence intensity.

**COMPLETED WITH CHANGES.** *The changes to this task did not involve changes in (i) methodology, (ii) stated objectives, or (iii) phenomena under study. Thus, prior approval was not obtained prior to making these changes.*

As discussed in AR#2, (experiment WA3, p13 and Figures 10 and 11), mixed population studies were not performed because such an experiment would have been trivial given the large differences we observed between MCF-7 WTC (AR#2 Figure 10) and MCF-7 ADR (AR#2 Figure 11) cell types. As stated in the AR#2 Conclusions (p. 20) we believe AR#2 experiment WA3 demonstrates that 1 MDR cell out of 1000 could easily be detected. Instead, we developed a graded series of MCF-7 ADR cell lines that had spent a variable amount of time in culture, in the absence of doxorubicin. As discussed above, the development of these cell lines required the development of high passage number (PN) MCF-7 WTC and MCF-7 ADR cells (Parissenti WTC and ADR cells, PN=27, and PN=23, respectively) representing a time in culture of 24 weeks. (see Appendix C, 2002 AACR abstract entitled, "A VSOM calcein assay for quantitation of multidrug resistance in human breast cancer cells", to be presented at the 93rd Annual Meeting of the AACR, San Francisco, April 6-10, 2002, Abstract ID 106867).

Also as discussed above in Task 3, the cellular responses we observed in these experiments were too slow for a human operator to sit and "interact" with the VSOM system. Thus, one important result of this project is our determination of the fact that automation of VSOM experiments is superior to manual operation because cellular responses are often too slow for a human operator to sit, observe, and interact with a "real-time" experiment. For human interaction, assessment, and verification these experiments needed to be speeded up after the experiment using time-lapse digital video sequences as discussed above in Task 3. The types of "decisions" that our current VSOM instrument currently makes is whether or not the specified (upper or lower) threshold intensity levels pre-programmed into the MainFrame Java GUI have been achieved (discussed above in Task 1). Pumps are then started or stopped on the basis of comparisons between these preset thresholds and the current calculated mean fluorescence intensity of single cells or populations of cells. The software ADR was used to perform successful automated experiments such as these, which were later verified off-line by a human operator. Once again, the difference between the MCF-7 WTC and MCF-7 ADR cell types were so large, it was deemed trivial to perform such studies on mixed populations of cells. Instead, we began development of a more challenging, graded series of MCF-7ADR cell lines with increasingly lower levels of Pgp expression (see Appendix C).

**Task 5:** Perform automated VSOM experiments and demonstrate computer controlled automated perfusion of verapamil. Compare to work of trained human operator.

**COMPLETED WITH CHANGES.** *The changes to this task did not involve changes in (i) methodology, (ii) stated objectives, or (iii) phenomena under study. Thus, prior approval was not obtained prior to making these changes.*

All of our verapamil and calcein perfusion studies are "automated" (no human operator need be present) and real-time "decisions" can be made via software control by referring to intensity thresholds preset in the Java GUI "MainFrame", as discussed above in Tasks 3 and 4. One important result of this project is our determination that "physiological fingerprints" obtained by perfusion and washout of CAM in the presence and absence of MDR modulators (**Figure 4**) reflect the amount and type of MDR proteins present in a given living cell. The particular pump recipe for generation of optimal physiological fingerprints need not be standardized, nor known ahead of time and a human operator need not be present. This automation is necessary and superior to manual operation because the cellular physiological responses observed are often very slow. **Figure 4C, F** are examples of VSOM-generated physiological fingerprints for late-passage (PN=23) MCF-7 ADR cells. As seen by comparing Figure 4A and Figure 4B, both MCF-7 WTC and high PN MCF-7 ADR cells accumulate intracellular calcein at similar rates. Large populations of cells shown the same behavior (Figures 4D,F). Early passage MCF-7 ADR cells accumulate little calcein during such CAM perfusion intervals, as discussed above.

**Technical Objective 2:** *Simultaneous observation and correlation of multiple physiological responses that may reflect separate and independent MDR mechanisms in MDR breast cancer cells.*

**Task 6:** Obtain transmitted light images of all cell types. **COMPLETED.** (discussed in AR#1 and AR#2).

**Task 7:** Perform manual mode VSOM (a) CAM plus verapamil assays (b) LTR plus monesin assays (c) FURA-PE3 calcium ratio imaging and viability studies.

### **COMPLETED WITH CHANGES.**

*The changes to this task did not involve changes in (i) methodology, (ii) stated objectives, or (iii) phenomena under study. Thus, prior approval was not obtained prior to making these changes.*

**Task 7a:** As seen in AR#2 (experiment WA3, page 13 and Figures 10 and 11), we successfully demonstrated the preferential retention of calcein in MCF-7 WTC cells, relative to MCF-7 ADR cells. In addition, **Figure 4F** shows the effect of verapamil on high PN MCF-7 ADR cells. As shown in Figure 4B, the MDR modulator verapamil is being perfused during pump interval F, near the 5000s time point. If one examines the peak fluorescence intensities in Figures 4C and F, one can see that the maximum amounts of calcein accumulation take place in high PN MCF-7 ADR cells when the Pgp inhibitor verapamil is present. A negligible effect of verapamil is observed in MCF-7 WTC cells (Figure D), which is to be expected since they contain little Pgp (see Appendix E, Figures 8G and H).

**HMEC cell lines:** HMECs were not included in the original proposal (OP). Because of (i) the great increase in the number of MCF-7 cell lines required for our MDR studies (Lupu DS and MDR cell lines, Parissenti DS and MDR cell lines, and high PN DS and MDR Parissenti cell lines), (ii) our participation in the important  $\beta$ -testing of the **MultiDrugQuant Assay Kit with MK-571**, and (iii) our requirement for MCF-7 fluorescence multiwell plate experiments, concomitantly fewer studies were performed using the HMEC cell lines from Dr. Yaswen. As discussed in AR#2 (Cytofluor experiment WA1, pp. 11-13), it was necessary to conduct multiwell plate experiments using a fluorescence plate reader, even though support for these experiments had been cut from the original proposal. Although flow cytometric studies would have been the preferred experimental technique for comparisons between VSOM and traditional assays, we had access to a Cytofluor 4000 fluorescence plate reader and for this reason made comparisons between VSOM and traditional multiwell plate assays. These experiments successfully demonstrated (AR#2) the increased sensitivity and other important advantages of VSOM assays relative to traditional multiwell plate assays.

**Task 7b:** As noted in preliminary results presented in AR#1 (page 7 and Figure 9), one of the VSOM assays we initially proposed (detection of acidification defects using LT-Red and monesin) was found to be unsuitable for VSOM instrument development, especially when used with the MCF-7 cells obtained from our colleague, Dr. R. Lupu. For this reason, we obtained a new set of matched cells (MCF-7 WTC and MCF-7 ADR cells from Dr. A. Parissenti) and focused solely on the second assay we proposed to study (Task 7a, detection of Pgp and MRP using calcein-AM and verapamil). For this reason, no further experiments were performed using the LT-Red assay(s) as proposed in Task 7b.

**Task 7c:** As discussed in AR#2 (**Experiment HM2**, pp. 16-17, Figures 16 and 17), several important calcium ratio imaging and FURA-PE3 experiments were performed using HMEC cell lines, as proposed. As discussed in AR#2 this work began with the proposed viability and baseline studies and rapidly progressed to the intracellular calcium and thapsigargin (TG) stimulation studies proposed for Task 9. As seen in Figures 16 and 17 of AR#2, we observed a very large response to TG (and the calcium ionophore ionomycin) in the **184B5 HMEC** cell line. These HMECs were loaded with the calcium-sensitive fluorescent probe FURA-PE3, and the compound LDS-751. LDS-751 initially localizes to cellular mitochondria and the cell nucleus, and this is one reason we attempted to use it as a counterstain. We had hoped to use its red fluorescence in the red channel for nuclear and cytoplasmic segmentation in much the same manner as we had used TMRE for cell detection and segmentation (Figure 5B, "I", **Appendix E**, Biophysical Society poster). In addition, LDS-751 is also useful as an indicator of apoptosis (See R.P. Haugland's "Handbook of Fluorescent Probes and Research Products" Section 8.1, Eighth Edition, 2001, Molecular Probes, Eugene OR, ISBN 0-9652240-8-2). Upon exposure to high levels of

intracellular calcium, LDS-751 escapes from the mitochondria (an early indication of apoptosis) and binds to mRNA. LDS-751 has unique fluorescence properties. When bound to double-stranded DNA, it excites at 543nm and emits at 712nm (near-IR), however, when bound to mRNA it excites at 590nm and emits at 607nm. In addition, when LDS-751 is bound to nuclear DNA, it appears bright red (non-fluorescent) in transmitted light images. All of these unique properties are potentially useful for multichannel detection and segmentation of cells, cross-channel detection and correlation of physiological events, and high resolution segmentation of the cell into its various subcompartments (nuclear, cytoplasmic, mitochondrial, etc. ).

We believe that the large LDS-751 response we observed to TG and ionomycin (AR#2, Figures 16 and 17) were due to an early event in apoptosis, i.e, the membrane permeability transition and depolarization of the mitochondria. One of our goals in the intracellular calcium ratio imaging Tasks was to make a correlation between intracellular calcium levels and the subsequent physiological events triggered by intracellular calcium signaling, such as apoptosis and proliferation. Thus, it became imperative to develop fluorescence assays for apoptosis and proliferation (as discussed below) before performing extensive intracellular calcium ratio imaging experiments.

However, as discussed in AR#2, we did perform several preliminary experiments (such as **Experiment HM2**) where we attempted to perform calcium ratio imaging with the FURA-PE3 fluorochrome and a second fluorochrome (such as LDS-751) which would not only serve as an indicator of a physiological event (apoptosis) but would also be used as counterstains for cell segmentation purposes. Several technical difficulties were encountered when attempting to perform intracellular calcium ratio imaging studies with LDS-751, Hoechst 33342, or Syto-16 as counterstains. The fluorescence excitation filters in our filter wheel are 340nm, 360nm, 380nm, 405, 490nm, and 570nm. The dichroic and barrier filter set used is the Pinkel triple bandpass set (Chroma Technology Corp, Brattleboro, VT, Set 8100). When using this filter set, any and all fluorescence emission in the wavelength bands of 440-460nm, 510-550nm, and 600-750nm are detected at the camera (assuming additional near-IR filters do not exist at the camera). Thus, when attempting to perform calcium ratio imaging at 340 and 380nm, one also excites the second fluorochrome to some extent. Although the fluorescence emission of the second fluorochrome may be "red", any and all fluorescence (blue, green, and red) is simultaneously detected at the camera. This made our calcium ratio imaging experiments very technically difficult.

Thus, after these initial HMEC experiments, and after consultation with our collaborators, we determined that development of fluorescence assays for proliferation, propagation, and apoptosis should take priority over, and be substituted for, the calcium regulation and calcium influx studies proposed in Task 7c and Task 9 (calcium influx post-TG stimulation - See Task 9, below).

**Task 8:** Simultaneous observation and correlation of two MDR mechanisms.

**COMPLETED WITH CHANGES.** *The changes to this task did not involve changes in (i) methodology, (ii) stated objectives, or (iii) phenomena under study. Thus, prior approval was not obtained prior to making these changes.*

The physiological fingerprints shown in **Figure 4** are an example of our "simultaneous observation and correlation of two MDR mechanisms" experiments. The two mechanisms observed are the separate activities of two different MDR proteins, Pgp and MRP. Although they share some of the same substrates, these transmembrane pumps have many differences, including differential inhibition of activity when exposed to certain inhibitors such as MK-571. In addition, these MDR proteins each have a unique molecular mechanism of activity and a unique (although somewhat overlapping) spectrum of substrates. As seen in **Figure 5A,B**, DS MCF-7 WTC cells have only MRP and no Pgp. They do, however, have high levels of Bcl-2 which is itself a form of resistance to apoptosis. MCF-7 ADR cells, on the other hand, have high levels of Pgp and low levels of MRP and Bcl-2. As noted in the key to **Figure 5A,B** and as illustrated in **Figure 5C**, Pgp and MRP operate differently on the CAM and CAL substrates and show differential sensitivity to the MRP inhibitor MK-571. Only MRP has the ability to pump CAL out of the cytosol after it has (passed through the cell membrane) been cleaved by intracellular esterases. Pgp intercepts CAM (only) while it is still in transit through the cell membrane, while

MRP can pump out cytosolic CAM. Verapamil has the ability to inhibit the operation of both Pgp and MRP, while MK-571 inhibits the operation of MRP only. Competitive inhibition occurs in both cases.

**Figure 5D** is a schematic diagram of a protocol designed to take advantage of these Pgp and MRP differences, in a way that allows one to calculate the presence or absence of each and the relative contribution each makes to cellular MDR. The VSOM protocol shown in Figure 5D was adapted from the flow cytometry protocol specified for the Solvo  $\beta$ -test MDR kit.

As seen in Figure 4B,C for individual cells and Figures 4D,F for large populations of surrounding cells, the VSOM protocol shown in Figure 5D and Figure 4B was able to demonstrate the existence and cooperative behavior of two separate MDR mechanisms for the efflux of foreign compounds such as CAL and CAM. In these high PN cells (which more similar to each other than the low PN cells, but are not fully characterized yet) one can clearly see that perfusion of CAM+MK-571 (pump interval "d") has a much smaller effect on MCF-7 ADR cells than does the inhibitor verapamil during pump interval "f" (CAM+VER). These two peaks indicate the amount of MDR contributed by MRP (peak of interval "d") relative to the overall MDR contributed by MRP and Pgp together (peak of interval "f"). This experiment is discussed in more detail in **Appendix G**, Section 2.7. The behavior exhibited by MCF-7 WTC cells is more difficult to interpret, and would benefit from numerical simulations of the MRP pump kinetics, as discussed in Appendix G, Section 2.7. Automated VSOM will allow us to optimize the extraction of more informative physiological fingerprints from MCF-7 WTC cells. For example, the same protocol and timings were used for both WTC and ADR cells for purposes of comparison; however, as seen from the small wash-out effect during intervals "c", "e", and "g" (Figure 4A), the wash-out intervals should have been extended in order to observe more significant dips in the intracellular CAL concentration. In addition, it may be advantageous to pre-expose the cells to MK-571 before perfusing CAM, and to maintain exposure to MK-571 during certain washout intervals. These experiments are proceeding, but at reduced effort since funding for them was discontinued over a year ago.

**Task 9:** Calcium influx studies after TG stimulation, and observation of alterations in calcium regulation that identify different breast cancer and different HMEC cell types

**COMPLETED WITH CHANGES.** *The changes to this task did not involve changes in (i) methodology, (ii) stated objectives, or (iii) phenomena under study. Thus, prior approval was not obtained prior to making these changes.*

As discussed in Task 7, we determined that development of VSOM fluorescence assays for proliferation, propagation, and apoptosis should take priority over, and be substituted for, the calcium regulation and calcium influx studies originally proposed in Task 7c and Task 9 (calcium influx post-TG stimulation). Some important TG stimulation studies were performed before making this decision, as discussed in Task 7.

As discussed on page 3 and page 7 of the AROP, the rationale for **Task 9** was our desire to find and exploit differences between cell types in order to to give a growth advantage to specified cells (i.e., primary breast tumor cells), while giving a growth disadvantage to other cells (i.e., normal mammary epithelial cells). It became apparent to us that VSOM assays for quantifying the physiological effects (apoptosis, proliferation, differentiation, cell detachment) of intracellular calcium signaling should be developed before detailed intracellular calcium signaling experiments.

It should be noted that in the OP, we originally proposed glucose deprivation/apoptosis studies on our MCF-7 model system. As seen below, we reinstated these experiments after performing initial TG stimulation studies of FURE-PE3 loaded HMEC cells (as discussed in Task 7).

Thus, as seen below, and as discussed in AR#2, we have begun to develop (i) VSOM assays for various stages of apoptosis, (ii) VSOM assays for cell attachment, and (iii) VSOM assays for cell proliferation. Continued improvement of these assays will allow us automatically and intelligently design the appropriate

microenvironmental conditions for the propagation of primary human breast tumor cells. This will be critical for our future goal of designing cancer therapy tailored to an individual breast cancer patient, because it is currently difficult to get breast cancer cells from tumor biopsies to grow in an artificial cell culture environment.

**VSOM Assays for Cell Proliferation and Attachment:** In AR#2 we discussed the results of our BrdU incorporation assays for proliferation in living HMECs (experiment HM1, Figures 7B,C,D), and our studies of the effects of pH on HMEC cell propagation and MCF-7 cell attachment in culture (Figures 13, 14). The BrdU incorporation fluorescence assay (Figure 7, EGF stimulation effects) and the pH morphometric assay (Figures 13 and 14; a morphometric assay based on transmitted light digital images) were not specifically included in our original proposal. However, these experiments together with new apoptosis fluorescence assays (presented herein) were judged by us and our collaborators (Dr. Paul Yaswen (LBNL), Dr. Shanaz H. Dairkee, (Geraldine Brush Cancer Research Institute, San Francisco), Dr. Amadeo Parissenti (North Eastern Ontario Regional Cancer Centre (NEORCC), Sudbury, Ontario) to be of critical importance for (i) future funding, (ii) future improvements in the propagation of tumor cells from primary breast cancer biopsies, (iii) current development of the new VSOM fluorescence (and transmitted light) assays that will be required for the development of improved cell culture techniques for propagation of tumor cells from primary breast cancer biopsies, and (iv) improvement of current *in vitro* fluorescence assays for MDR. As stated in the AROP (Discussion section), "Our objectives are to develop the VSOM in a stepwise fashion and gather preliminary data to aid future development of cell culture techniques and fluorescence assays...Additional funding will required for these future projects." Also stated in the AROP, (HMEC Model Cell System section), "Depending on the cell type and the final  $[Ca^{2+}]_i$ , proliferation, differentiation, or apoptosis could then be selectively induced in that type of cell."

Further explanation of this rationale was presented in our June 2000 DoD BCRP grant proposal BC000508, entitled "Rapid Discovery of Physiological Characteristics Which Distinguish Malignant and Nonmalignant Human Breast Epithelial Cells" (Callahan, Parvin, and Dairkee, co-PIs. Funding for this research was not approved.). A copy of this proposal is found in AR#2 (Appendix G, pgs 76-95).

**VSOM assays for apoptosis:** We have begun to develop VSOM assays for apoptosis. This complements our previous work on (i) cell attachment as a function of pH, and (ii) cell proliferation as a function of EGF stimulation. **Figure 6** is an example of apoptosis induced by glucose deprivation. These cells are in an intermediate phase of apoptosis, where they have begun to round up and detach from the surface (Figure 6A). Only a portion of the cells are dead, as seen from the fact that only some of the cell nuclei (all cell nuclei in Figure 6B are labeled with H42, a blue nuclear stain for living and dead cells) are labeled with EthD-1 (a red fluorescent nuclear stain for dead cells with compromised cytoplasmic membranes) in Figure 6D. Figure 6C demonstrates the binding of FITC-conjugated anti-Annexin V to the outer membrane of both dead and living cells. The presence of Annexin V on the outer surface of living cells is an early sign of apoptosis. Note that some signal from EthD-1 staining bleeds through into the green channel (Figure 6C). This is a technical difficulty associated with our use of the Pinkel triple bandpass filter set, as described earlier.

## **Key Research Accomplishments during Final No-Cost Extension Year**

- **Developed and tested new JAVA GUI, "MainFrame"**
- **Developed new software to track cell motion during VSOM**
- **Demonstrated VSOM apoptosis fluorescence assays**
- **Demonstrated high resolution VSOM using CSMI microperfusion chamber**
- **Demonstrated VSOM "physiological fingerprints" for MDR phenotypes**
- **$\beta$ -tested commercial MDR assay kit and modified it for VSOM**
- **Initiated and attempted to fund new collaborations with Cancer biologists**

## **Reportable Outcomes for Year 3**

### **Abstracts and Presentations (included in Appendices B and C):**

1. Callahan, D.E., and Parvin, B. **A VSOM calcein assay for quantitation of multidrug resistance in human breast cancer cells.** *To be presented at the 93rd Annual Meeting of the AACR, San Francisco, April 6-10, 2002, ABSTRACT ID 10686.*
2. Callahan, D.E., and Parvin, B. **BioSig: A Database for Efficient VSOM Extraction of Dynamic Phenotypic Data from Individual Living Cells** *to be presented in a Platform Session (Session Title: Platform S - Biophysical Chemistry & Emerging Techniques, Monday, February 25, 2002) at the Biophysical Society Annual Meeting in San Francisco, California, February 23-27, 2002 (Program #860-Plat).*

### **VSOM Grants Funded:**

#### **Automated Imaging System for Guiding Antisense Compounds to Specific mRNA Targets in Living Cells**

Co-PIs: Parvin, B., Callahan, D.E. (See **Appendix G, AR#2**, currently in Year 2)

Funded through the Office of Biological and Energy Research, Molecular Nuclear Medicine Program "Imaging Gene Expression in Health and Disease", in the Office of Science, U.S. Department of Energy, under contract DE-ACO3-76SF00098.

Amount: \$1.2M total, 3 years

### **VSOM Grants Submitted and Not Funded :**

#### **In Vitro Simulation of Breast Tumor Cell Microenvironments (Included in Appendix H)**

Co-PIs: Parvin, B., Callahan, D.E.

Submitted to: California Breast Cancer Research Program

Date: January, 2001

Type: "STEP Award, Innovative Treatment Modalities",

Amount Requested: \$232K total, 2 years

#### **Predictive Models from Subcellular Physiological Responses (Included in Appendix G)**

Co-PIs: Parvin, B. and Callahan, D.E.

Date: October, 2001

Submitted to: the Joint DMS/NIGMS Initiative (NSF 01-128)

Amount Requested: \$2.45 million total, 5 years

### **Patent Application (included in Appendix D)**

U.S. Patent Application, VSOM Methods and Devices, PCT/US01/18382 (LBL-06259)

### **Technology Transfer:**

The LBNL Technology Transfer Office is entering into a licensing agreement with an outside company that will facilitate commercial VSOM development. This license will be for the technology contained in the *Visual Servoing Optical Microscopy* patent application. The company, "Bioselect, LLC", is located in St. Louis, MO. The effective date of this agreement is expected to be early in 2002.

## Conclusions

The ultimate goal(s) of our research are to (i) develop an instrument, software, and bioinformatics infrastructure that will allow us to (ii) develop improved *ex vivo* fluorescence assays such as assays for microenvironment design, drug response and multidrug resistance, and (iii) improve primary tumor cell culture microenvironments so that tumor cells freshly derived from the solid tumors of individual breast cancer patients can be successfully propagated and tested *ex vivo*.

The VSOM demonstrations we present here clearly show the feasibility and advantages of VSOM MDR assays. We have demonstrated a rapid VSOM fluorescence assay for doxorubicin chemosensitivity that can identify a subpopulation of cells in a much larger population of cells. In this VSOM fluorescence assay, for this model cell system, optimizing the retention of calcein is equivalent to optimizing the uptake and cytotoxicity of the anticancer drug doxorubicin. It appears unlikely that a single MDR kit, single set of inhibitors, single set of concentrations and exposure times will be able to deal with the wide range of MDR proteins that are overexpressed to varying extents in multidrug resistant tumor cells. VSOM technology offers the advantage of intelligent adaptation during ongoing quantification of dynamic cell responses. This means that an assay could be modified on-line, intelligently and automatically, on a specimen-by-specimen, or patient-by-patient basis. The number and type of exposures, the order and duration of exposures, the compounds and the concentrations used can be optimized during the assay in order to efficiently and rapidly obtain the physiological information necessary to select the best chemotherapeutic drugs for that patient. We believe we have demonstrated that 1 MDR cell out of 1000 DS cells can easily be detected and stimulated repeatedly, for hours, in order to determine the number and type of MDR proteins expressed at the cell surface. Thus, we believe we have demonstrated the technical feasibility of *ex vivo*, VSOM assays that could be used to design breast cancer chemotherapy for the individual patient.

In addition, our preliminary work on VSOM fluorescence (and transmitted light) assays for cell attachment, proliferation, and apoptosis show promise for the future development of improved cell culture techniques that will allow propagation of tumor cells from primary breast cancer biopsies. We hope to use VSOM for automated design of microenvironments that favor the propagation of primary human breast tumor cells. This will be critical for our future goal of designing cancer therapy tailored to an individual breast cancer patient, because it is currently difficult to get breast cancer cells from tumor biopsies to grow in an artificial cell culture environment.

Several aspects of our approach are novel. We have combined sophisticated robotic vision techniques, digital video microscopy and biophysics to monitor and automatically respond to the responses of hundreds of living cells. We have successfully demonstrated VSOM technology by analyzing the heterogeneity and physiological characteristics of large populations of drug-sensitive (DS) and multidrug resistant (MDR) human breast cancer cells in real-time. This demonstrates the advantages of a VSOM doxorubicin chemosensitivity assay based on the dynamic physiological responses of single cells. These results indicate our approach will be extremely useful for developing new VSOM chemosensitivity fluorescence assays for a variety of breast cancer drugs.

We hope to use VSOM in future studies to rapidly analyze large populations of living cells that have been freshly derived from human breast cancer tissue biopsies. This could lead to rapid advances in *ex vivo* chemosensitivity testing and would represent a large step toward our ultimate goal of chemotherapy regimens tailored to the individual breast cancer patient. We believe the rapid analysis of dynamic physiological responses on a patient-by-patient, tumor-by-tumor, and cell-by-cell basis will provide critical information for individualized cancer chemotherapy. Such assays could produce detailed and distinct physiological fingerprints that are highly predictive of an individual patient's response (both normal and tumor cell response) to a particular anti-cancer drug, particular combination of drugs, or particular sequence of drug exposures.

The future potential of VSOM technology has been elaborated on in our recent VSOM patent application (included in **Appendix D**). The current project supported only a very limited demonstration of VSOM technology. We have demonstrated that VSOM has the potential to couple intelligent, automated, and responsive

perturbations of the biological microenvironment with the ongoing analysis of living cells in real time. In addition, VSOM has been integrated into a bioinformatics framework. In the future, adaptive, responsive, and intelligent control of applied perturbations and stimuli will benefit greatly from real-time access to an on-line database of previously observed cell responses and biological outcomes. Algorithms have been developed and applied to detect and measure responses not only of the entire cell, but also of specific subcompartments within living cells. Temporal responses have been obtained from multichannel subcellular responses using a variety of fluorescent probes for living cells, and the relevant medical problem of multidrug resistance in living human cancer cells has been studied. In addition, the groundwork for connecting VSOM-evoked physiological responses to biological endpoints that may not develop for weeks to days has been laid.

We have assembled a list of current prices for a second, completely independent, improved and dedicated VSOM prototype that could be assembled for approximately \$100,000. We are currently working on a licensing agreement for commercial development of VSOM instruments, which should drop in price after additional technology development and price/performance evaluations. Our current work was performed on a shared Life Sciences Division automated microscope, digital camera, and host computer (purchased with funds from other funding sources), and many VSOM components had to be disassembled after each experiment, so that VSOM peripherals did not interfere with use of the microscope by other users. This severely limited our productivity. One current technical problem in setting up the second prototype is the fact that our current VSOM host computer is a SUN workstation, running the Solaris Operating System (OS, a flavor of the UNIX OS). Modern digital cameras do not provide driver support for the SUN S-BUS or Solaris OS. Thus, the LBNL Technology Transfer Office is currently negotiating with an outside company (BioSelect, LLC, St. Louis, MO) to license this technology and port the software to the Microsoft (MS) Windows 2000 OS. In addition, our current OBER VSOM grant is providing some funding support for the hardware required to set up a second, independent, dedicated VSOM prototype and the development of additional cell segmentation software and bioinformatics support.

**FUTURE WORK:** As discussed in the patent application in **Appendix D**, extensive additional development is required to realize the full potential of VSOM technology. For example, knowledge-based, real-time machine "intelligence" has not yet been developed, and remote operation with real-time deposition of digital data in a remote database is not yet fully functional. Thus, real-time searching of a remote database for comparisons of currently observed cell responses to previously observed cell responses (and subsequent biological outcomes) is not yet possible. The patent also describes multi-field VSOM operation (which implies autofocusing, stage control and sophisticated, on-line cell tracking) but funding for this capability was cut from the original proposal (OP); thus, it is currently not available. However, it is likely that BioSelect, LLC will choose to develop multi-field VSOM within one to two years of being granted a license to VSOM technology. Additional commercial development will depend on the degree of patent protection granted by the US Patent Office.

## References

1. Karaszi, E., et al., *Calcein assay for multidrug resistance reliably predicts therapy response and survival rate in acute myeloid leukaemia*. British Journal of Haematology, 2001. **112**(2): p. 308-14.
2. Legrand, O., et al., *Pgp and MRP activities using calcein-AM are prognostic factors in adult acute myeloid leukemia patients*. Blood, 1998. **91**(12): p. 4480-8.
3. Paul, D. and K.H. Cowan, *Drug Resistance in Breast Cancer*, in *Breast Cancer: Molecular Genetics, Pathogenesis, and Therapeutics*, A.M. Bowcock, Editor. 1999, Humana Press Inc: Totowa, NJ. p. 481-517.
4. Schindler, M., et al., *Defective pH regulation of acidic compartments in human breast cancer cells (MCF-7) is normalized in adriamycin-resistant cells (MCF-7adr)*. Biochemistry, 1996. **35**(9): p. 2811-7.
5. Mechetner, E., et al., *Levels of multidrug resistance (MDR1) P-glycoprotein expression by human breast cancer correlate with in vitro resistance to taxol and doxorubicin*. clin cancer res, 1998. **4**(2): p. 389-98.
6. Holló, Z., et al., *Calcein accumulation as a fluorometric functional assay of the multidrug transporter*. Biochimica Et Biophysica Acta, 1994. **1191**(2): p. 384-8.
7. Essodaigui, M., H.J. Broxterman, and A. Garnier\_Suillerot, *Kinetic analysis of calcein and calcein-acetoxymethylester efflux mediated by the multidrug resistance protein and P-glycoprotein*. Biochemistry, 1998. **37**(8): p. 2243-50.
8. Feller, N., et al., *Functional detection of MDR1/P170 and MRP/P190-mediated multidrug resistance in tumour cells by flow cytometry*. British Journal of Cancer, 1995. **72**(3): p. 543-9.
9. Hollo, Z., et al., *Parallel functional and immunological detection of human multidrug resistance proteins, P-glycoprotein and MRP1*. Anticancer Research, 1998. **18**(4C): p. 2981-7.
10. Budworth, J., T.W. Gant, and A. Gescher, *Co-ordinate loss of protein kinase C and multidrug resistance gene expression in revertant MCF-7/Adr breast carcinoma cells*. British Journal Of Cancer, 1997. **75**(9): p. 1330-5.
11. Thaden, J. and P.S. Miller, *Photoaffinity behavior of a conjugate of oligonucleoside methylphosphonate, rhodamine, and psoralen in the presence of complementary oligonucleotides*. Bioconjugate Chemistry, 1993. **4**(5): p. 386-94.
12. Chin, D.J., et al., *Rapid nuclear accumulation of injected oligodeoxyribonucleotides*. new biologist, 1990. **2**(12): p. 1091-100.
13. Thierry, A.R. and A. Dritschilo, *Intracellular availability of unmodified, phosphorothioated and liposomally encapsulated oligodeoxynucleotides for antisense activity*. nucleic acids research, 1992. **20**(21): p. 5691-8.
14. Leonetti, J.P., et al., *Intracellular distribution of microinjected antisense oligonucleotides*. proceedings of the national academy of sciences of the united states of america, 1991. **88**(7): p. 2702-6.
15. Dickson, R.B. and M.E. Lippman, *Cancer: principles and practice of oncology*. Cancer of the Breast, ed. V.T. Devita, Jr., Hellman, S., and Rosenberg, S.A. 1997, Philadelphia: Lippincott-Raven. Ch. 36, pp. 1541-1557.
16. Cotter, T.G., et al., *The induction of apoptosis by chemotherapeutic agents occurs in all phases of the cell cycle*. Anticancer Research, 1992. **12**(3): p. 773-9.
17. Adams, J.M. and S. Cory, *The Bcl-2 protein family: arbiters of cell survival*. Science, 1998. **281**(5381): p. 1322-6.
18. Finkel, E., *Does Cancer Therapy Trigger Cell Suicide*. Science, 1999. **286**(17 December): p. 2256-2258.
19. Lowe, S.W. and A.W. Lin, *Apoptosis in cancer*. Carcinogenesis, 2000. **21**(3): p. 485-95.

20. Biroccio, A., et al., *bcl-2 inhibits mitochondrial metabolism and lonidamine-induced apoptosis in adriamycin-resistant MCF7 cells*. International Journal of Cancer, 1999. **82**(1): p. 125-130.
21. Reed, J.C., *Bcl-2: prevention of apoptosis as a mechanism of drug resistance*. hematology/oncology clinics of north america, 1995. **9**(2): p. 451-73.
22. Hengartner, M.O., *The biochemistry of apoptosis*. Nature, 2000. **407**(12 October): p. 770-776.
23. Zhang, L., et al., *Role of BAX in the Apoptotic Response to Anticancer Agents*. Science, 2000. **290**(3 November): p. 989-992.
24. Sakakura, C., et al., *Overexpression of bax sensitizes human breast cancer MCF-7 cells to radiation-induced apoptosis*. International Journal Of Cancer, 1996. **67**(1): p. 101-5.
25. Raynaud, F.I., et al., *Pharmacokinetics of G3139, a phosphorothioate oligodeoxynucleotide antisense to bcl-2, after intravenous administration or continuous subcutaneous infusion to mice*. Journal of Pharmacology and Experimental Therapeutics, 1997. **281**(1): p. 420-427.
26. Nicholson, D.W., *From bench to clinic with apoptosis-based therapeutic agents*. Nature, 2000. **407**: p. 810-815.
27. Waters, J.S., et al., *Phase I clinical and pharmacokinetic study of bcl-2 antisense oligonucleotide therapy in patients with non-Hodgkin's lymphoma [see comments]*. Journal of Clinical Oncology, 2000. **18**(9): p. 1812-23.
28. Schlagbauer-Wadl, H., et al., *Bcl-2 antisense oligonucleotides (G3139) inhibit Merkel cell carcinoma growth in SCID mice*. Journal of Investigative Dermatology, 2000. **114**(4): p. 725-30.
29. Cotter, F.E., J. Waters, and D. Cunningham, *Human Bcl-2 antisense therapy for lymphomas*. Biochimica Et Biophysica Acta, 1999. **1489**(1): p. 97-106.
30. Jansen, B., et al., *bcl-2 antisense therapy chemosensitizes human melanoma in SCID mice*. Nature Medicine, 1998. **4**(2): p. 232-4.

**Appendix A: Figures with Legends**

Pump Id	Syringe Id	Unit	Start time	duration	Off time	modulate	rate	Compound	Washout	concentration	con unit
0	0	MM	20	1800	0	off	0.5	BUFF	True	7.4	pH
0	1	MM	1830	1800	0	off	0.5	F-03139	False	0.1	F03139
0	0	MM	2630	1800	0	off	0.5	BUFF	True	7.4	pH
-1	1	MM	2430	1800	0	off	0.5	BUFF-VER	True	25	VER
-1	0	MM	7230	1800	0	off	0.5	F-03139...	False	25	VER
0	0	MM	6030	1800	0	off	0.5	BUFF	True	7.4	pH

Enter the number of Recipes you wish to enter:

Pump Scheduler | Scope Scheduler | I/O

Sample Rate:  Sec

Duration:  Sec

Filter:  1  2  3  4  5  6  7

Exposure (minutes):

Display Channel:  1  2  3  4  5  6

Dark Current Factor of:  Per time point  Once  Number of Frames Per Sec

Pump Scheduler | Scope Scheduler | I/O

Modulation of F-03139 uptake in ADR cells using Verapamil

Dish Comment

Dish Type:

Cell Type:

Media Name:

Volume (ml):

Concentration:

Oil Type:

Scope Parameter

Model:

Magnification:

Image Path Name:

Base File Name:

PumpScheduler File Name:

ScopeScheduler File Name:

PROPRIETARY

**Figure 1:** The VSOM Java GUI "MainFrame" is composed of 3 tabbed sections, or pages, called (A) Pump Scheduler, (B) Scope Scheduler, and (C) I/O. This VSOM GUI allows a user to specify a "recipe" and control the perfusion of compounds into a temperature regulated microperfusion chamber. In the Pump Scheduler, the columns "OFF-TIME", and "MODULATE" allow the user to tell the system how to adapt to real-time observations of cell responses. For example, if any cell within a field of cells reaches a specified mean fluorescence intensity (representing an intracellular calcein concentration) then the specified pump interval will end prematurely when the specified upper or lower threshold is reached. On the other hand, if the threshold is never reached within the allotted time, then the system will move on to the next perfusion interval regardless of the current state of the living cells. This automatic, responsive behavior can rescue many long term (overnight, for example) experiments that otherwise might need to be repeated.

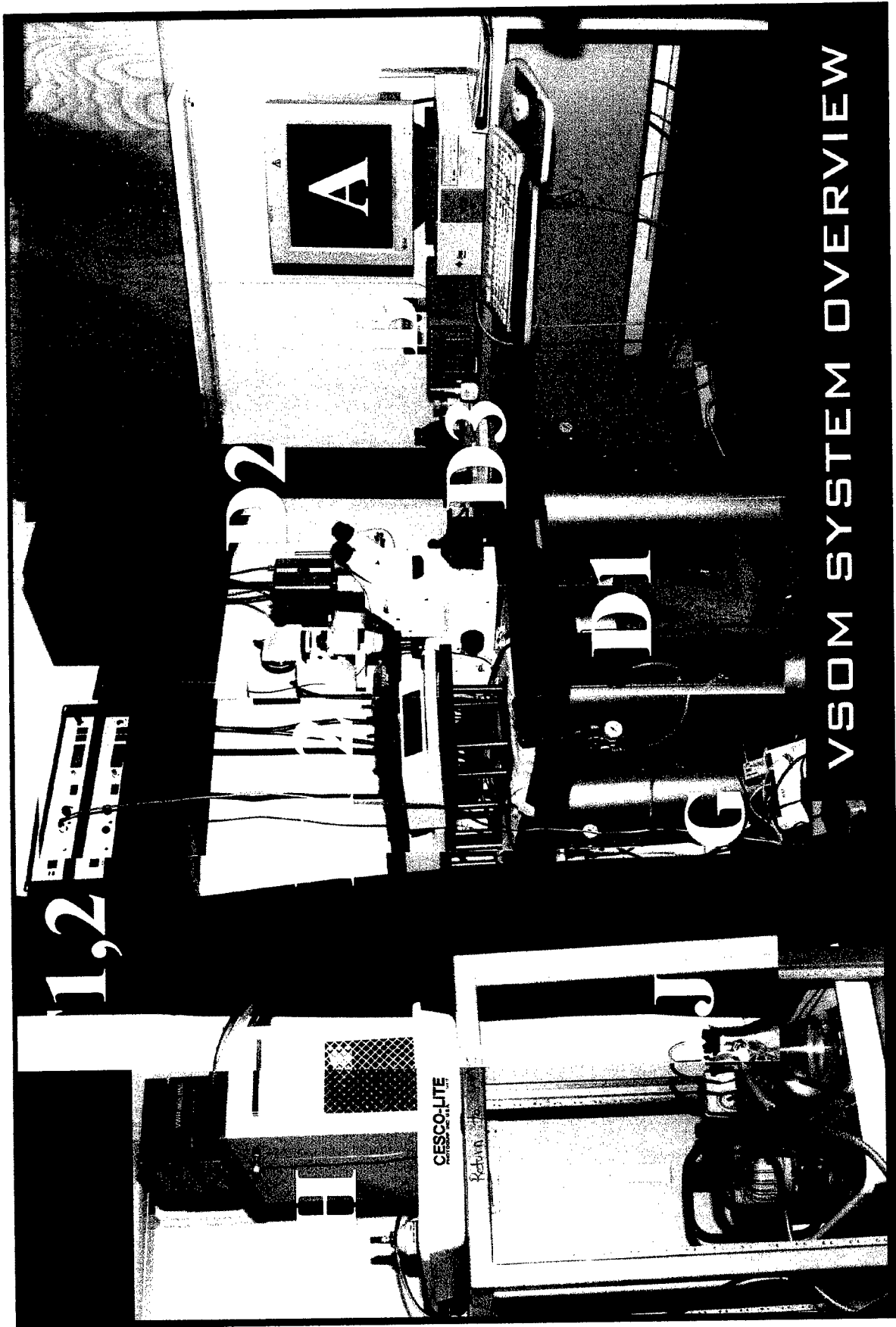
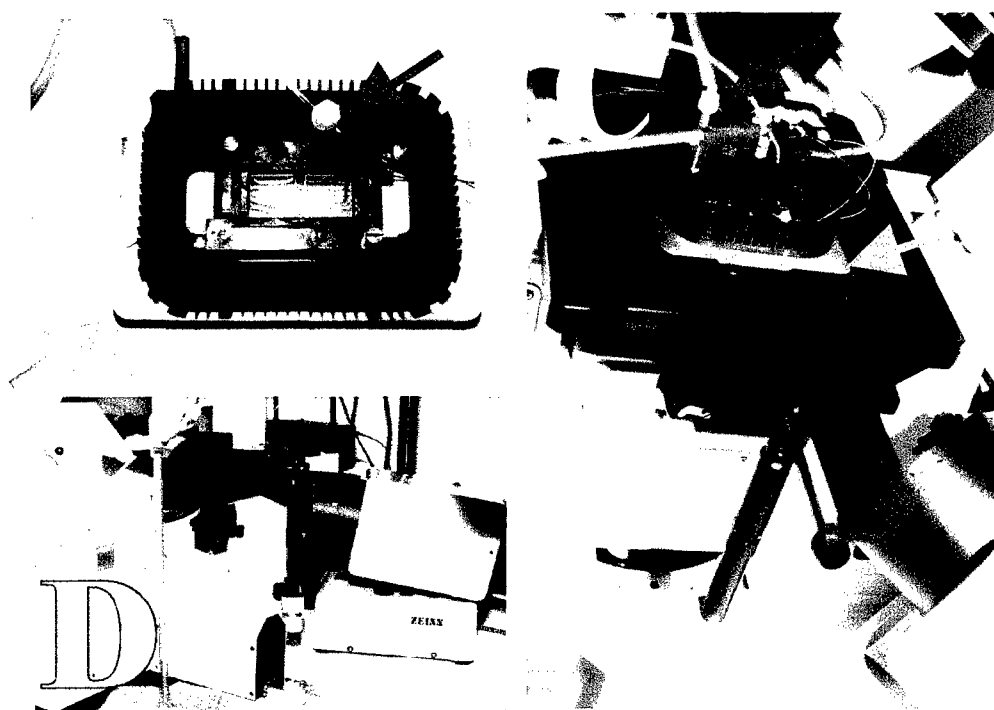


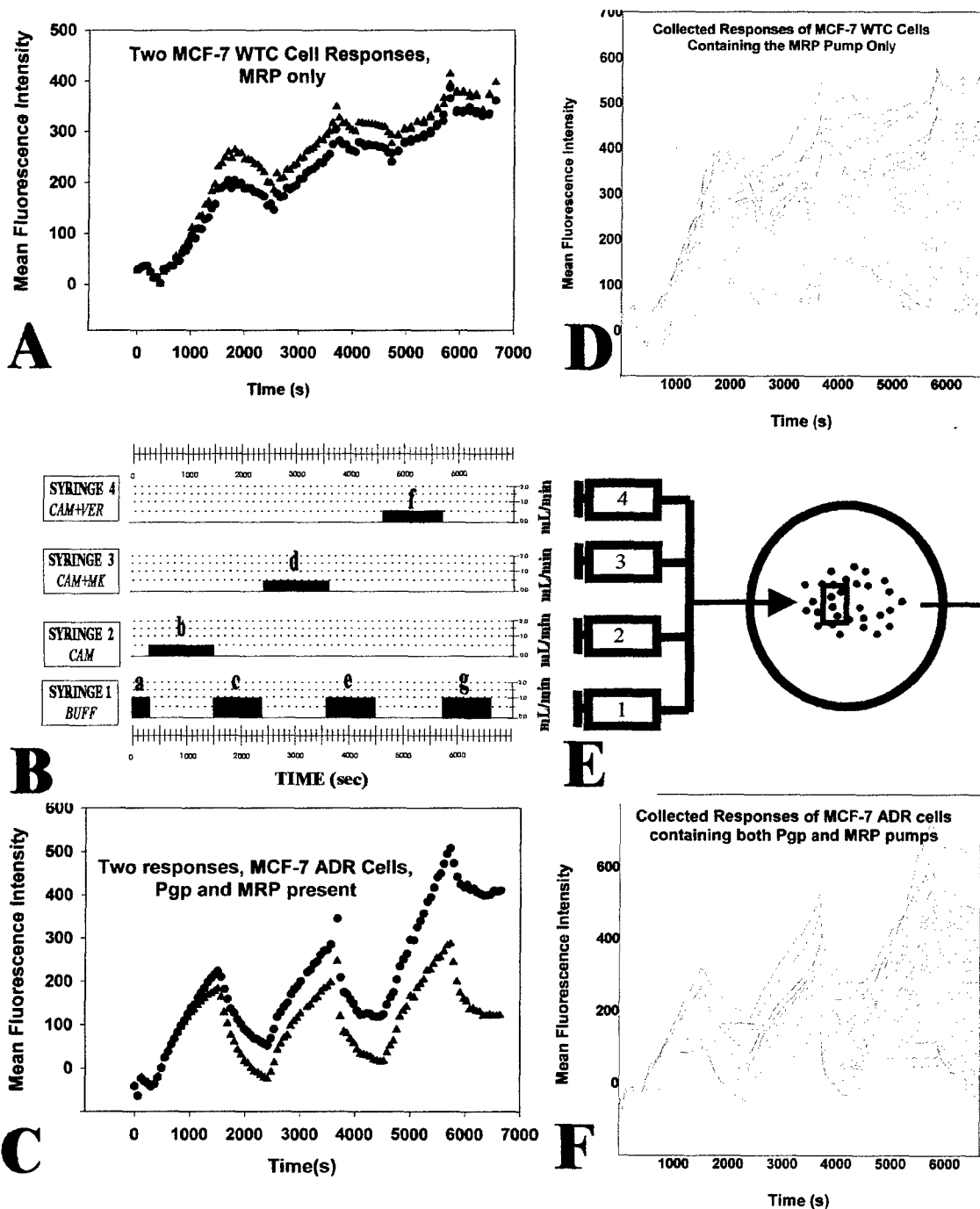
**Figure 2: VSOM SYSTEM OVERVIEW.** (A) SUN Workstation containing S-BUS SDV interface card for the Xillix digital camera and an S-BUS card with multiple serial ports, (B) LEP Controller for filter wheel, shutters, z-axis stepper motor, and x,y scanning stage, (C) Zeiss Axiovert 135TV inverted microscope with base port equipped for fluorescence and transmitted light (phase and DIC) microscopy, (D1) Xillix digital camera mounted on base port beneath microscope, (D2) upper port digital camera, (D3) standard 35mm camera, (E1,2) Two dual-syringe, computer-controlled (serial port) Harvard syringe pumps, (F1,F2) Two Harvard microperfusion chamber temperature control units, (G) 100BaseT Ethernet connection, (H) circulating water pump for additional heating or cooling of cell chamber, (I) Vacuum pump for cell chamber fluid aspirator, (J) Vacuum flask to collect aspirated fluid.

**PROPRIETARY**



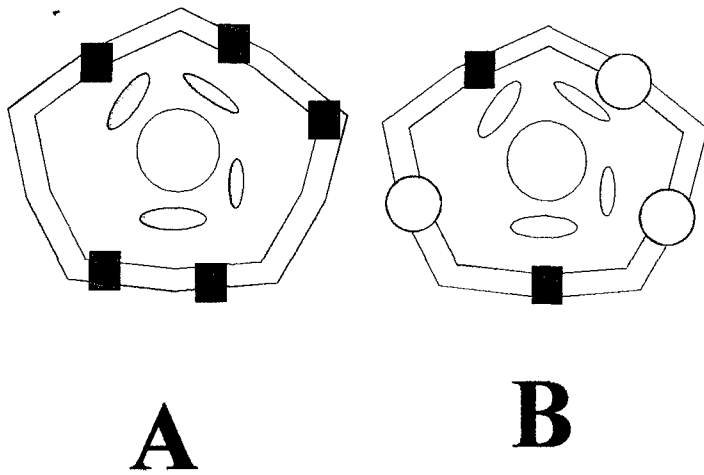
PROPRIETARY

**Figure 3:** Harvard CSMI Cell Chamber for Chambered Coverslips. (A) For improved optical resolution and fluorescence emission detection, we have moved to the use of chambered coverslips. The chamber volume can be controlled via the use of single, double, quad, etc. chambers per coverslip. Additional control of the chamber volume is through adjustment of the height of the vacuum aspirator (Red Arrow in B and C). A Harvard CSMI microperfusion chamber was modified as shown in (B). An aluminum stage plate insert (Green Arrow in B and C) was coupled to the CSMI so that the CSMI could be mounted on a Zeiss mechanical stage. This standard size insert also allows the CSMI to be mounted on the LUDL computer-controlled xy scanning stage described in previous Annual Reports. A bath-type thermistor BSC-T3 (Blue Arrow in B) is placed in the perfusion chamber and reports current temperature readings to the Harvard Apparatus TC-202 bipolar temperature controller. This controller delivers and adjusts current to Peltier devices in the microincubator. However, as shown in (D) it was necessary to also employ an Nevtek ASI-400 Air Stream Incubator (D, below and to the right of the microscope stage) in order to maintain a chamber temperature of  $37^{\circ} \pm 0.2$  C during constant perfusions. A ring stand was used to suspend the BSC-T3 thermistor in the active perfusion chamber.



PROPRIETARY

Figure 4: VSOM-Generated Physiological Fingerprints of MDR in two different cell lines. Data reprocessed with improved software. (A) Calcein-AM uptake, conversion to calcein, and retention in two MCF-7 WTC cells. The combined responses of all cells in the field of view are shown in D. MCF-7 WTC cells express the MRP transport pump only. (B) The perfusion intervals (the "recipe") used to generate the uptake and retention curves shown in A, C, D, and F. The composition of each of four syringes is indicated, as is the sequence and duration of each interval and the rate of perfusion during each interval. The time axes of A, B, and C are aligned for easy comparison of perfusion intervals and cell responses. (C) Calcein-AM uptake, hydrolysis to calcein, and retention in two MCF-7 ADR cells. The combined responses of all cells are shown in F. MCF-7 ADR cells express both Pgp and MRP transport pumps. (E) Schematic diagram indicating perfusion from four syringes into a microperfusion chamber. The gray box indicates one microscopic field of view, and indicates that only a subpopulation of all cell responses within the chamber are plotted in A, C, D, and F.



○ High bcl-2 mitochondrion

○ Low bcl-2 mitochondrion

■ **MRP:** Pumps Calcein out of Cytosol, and pumps Calcein-AM out of plasma membrane. It is inhibited by both MK-571 and Verapamil.

○ **Pgp:** Pumps Calcein-AM out of plasma membrane, and is inhibited by Verapamil

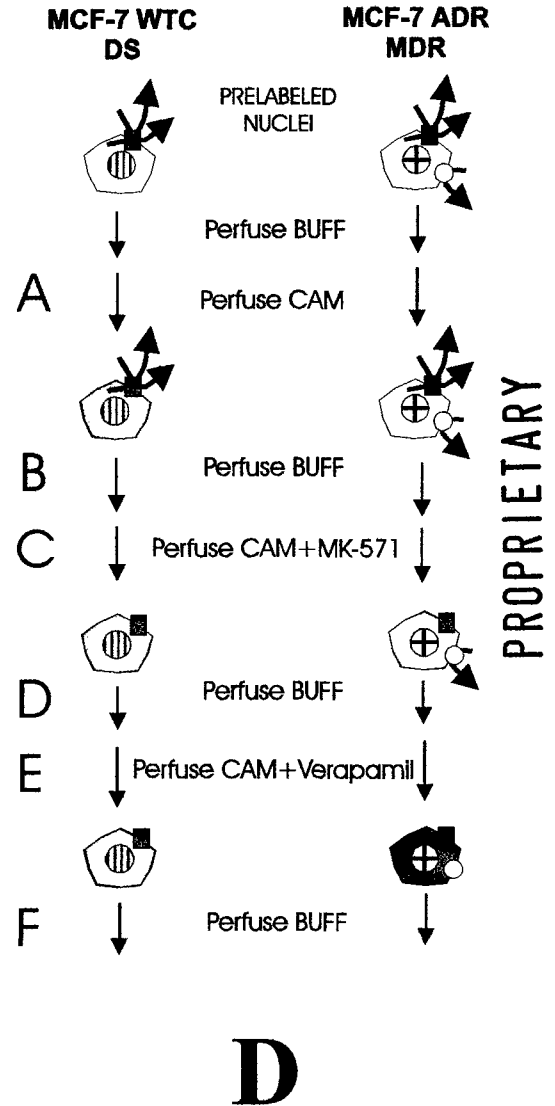
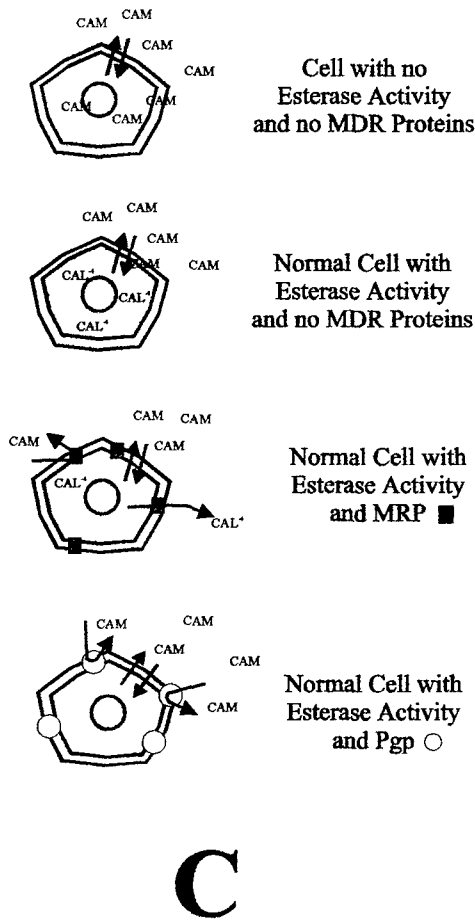


**Figure 5:** The MCF-7 WTC and the MCF-7 ADR Model cell system (A) Drug Sensitive MCF-7 WTC cells have high levels of the MDR membrane pump MRP, high levels of Bcl-2, and no Pgp (B) Multidrug resistant MCF-7 ADR cells have high levels of Pgp, low levels of MRP and Bcl-2 (C) Conversion of CAM to CAL (green shading, fluorescent calcein) via intracellular esterases, and the different efflux mechanisms of Pgp and MRP (D) flow chart of the VSOM pump intervals, or "recipe" used to generate the physiological fingerprints in Figure 4. DS, drug sensitive; MDR, multidrug resistant. Blue shading indicates Hoechst 33342 conterstain.

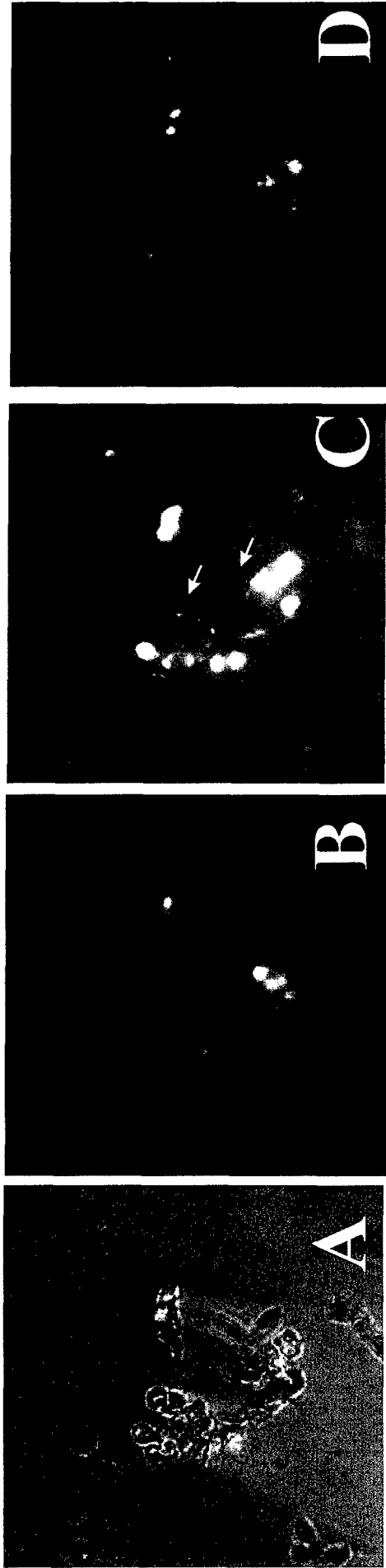


**Figure 6:** Glucose-deprivation induced apoptosis in MCF-7 ADR cells. Cells were exposed to media lacking (i) phenol red (ii) bicarbonate buffer, or (iii) glucose. 10% dialyzed fetal bovine serum (FBS) was present, which contains very low levels of glucose. Cells were exposed for 24h at 37 C, and then four channel digital images were acquired. (A) Transmitted light image of the morphological changes characteristic of apoptosis (B) Blue Hoechst 33342 channel. Nuclei of both living and dead cells are stained. (C) Green Annexin V channel image of cells stained with an FITC-conjugated anti-Annexin V antibody (Molecular Probes, Eugene, OR). Cells in the early stages of apoptosis exhibit a 3D shell of Annexin V membrane staining (arrows) (D) Ethidium homodimer I (EthD-1) nuclear staining of the subset of cells that are dead.

PROPRIETARY

**Appendix B: Abstract, 2002 Annual Meeting Biophysical Society**

This abstract, entitled "BIOSIG: A DATABASE FOR EFFICIENT VSOM EXTRACTION OF DYNAMIC PHENOTYPIC DATA FROM INDIVIDUAL LIVING CELLS" has been scheduled in a Platform Session (Session Title: Platform S - Biophysical Chemistry & Emerging Techniques, Monday, February 25, 2002) at the Biophysical Society Annual Meeting in San Francisco, California, February 23-27, 2002 (Program #860-Plat).

**BIOSIG: A DATABASE FOR EFFICIENT VSOM EXTRACTION OF DYNAMIC PHENOTYPIC DATA FROM INDIVIDUAL LIVING CELLS.**

We are populating an object-oriented database (BioSig<sup>1</sup>) with (i) multi-channel, single cell physiological responses to applied perturbations, and (ii) specific biological endpoints that can be mapped, with high predictive power, to specific physiological responses of individual cells. BioSig has been designed for use with Visual-Servoing Optical Microscopy (VSOM)<sup>2,3</sup>. The data model and instrumentation have been tested. Calcein accumulation and retention in drug-sensitive (DS) and multi-drug resistant (MDR) cells was monitored during perfusions and wash-outs of calcein-AM in the presence or absence of MDR modulators MK-571 or verapamil. Distinct "physiological fingerprints" were obtained for DS and MDR cell phenotypes. Biological endpoints that have been monitored in living cells include proliferation (via BrdU incorporation and Hoechst 33342/Syto-16 image ratioing techniques) and several stages of apoptosis. 1. Parvin, B. et al. IEEE Int. Symposium on Cluster Computing and the Grid, (2001) pp. 48-55. 2. Callahan, D.E. & Parvin, B. Proceedings: Era of Hope Department of Defense Breast Cancer Research Program Meeting (2000) p. 709. 3. Callahan, D.E. & Parvin, B. Biophysical J. (2001) **80** 169a. *Funded by Department of Defense, DAMD17-98-1-8177 & U.S. Department of Energy DE-ACO3-76SF00098.*

**Appendix C: Two Abstracts for 2002 AACR Meetings**

**1. A VSOM calcein assay for quantitation of multidrug resistance in human breast cancer cells.** Callahan, D.E., Parvin, B. *To be presented at "A VSOM calcein assay for quantitation of multidrug resistance in human breast cancer cells", to be presented at the 93rd Annual Meeting of the AACR, San Francisco, April 6-10, 2002, ABSTRACT ID 106867*

**2. Bcl-2 mRNA as a Target for Antisense Imaging Agents: Digital Imaging Fluorescence Microscope Studies of F-G3139, a Fluorescently-labeled Phosphorothioate.** Callahan, D.E., Parvin, B.<sup>1</sup>, and Taylor, S.E., Life Sciences Division and <sup>1</sup>National Energy Research Scientific Computing Center, Lawrence Berkeley National Laboratory, 1 Cyclotron Road, Berkeley, CA 94720. *To be presented at "Molecular Imaging in Cancer: Linking Biology, Function, and Clinical Applications In Vivo". An AACR Special Conference in Cancer Research, January 23-27, 2002, Lake Buena Vista, FL.*

Attached is a document containing your submitted abstract. Please print a copy of this proof, mark the printout with your corrections, and fax the corrected proof page to 800-830-2586 (U.S.) or 617-621-1423 (international). Only typographical errors may be corrected at this time. **Do not rewrite the text in any way.** In particular, please review the author listing/spelling and any special characters used. If you find an error in a special character, draw the intended character AND one or more characters that could be substituted if we cannot typeset the intended character. If you prefer, spell the name of the character or symbol. For example: Alpha. Also note that your title should be in sentence case (capitalize only the first letter of the first word in the title with the exception of any abbreviations: e.g., Differential prostate tumor RNA and protein expression in the HER kinase axis: In vitro versus in vivo). If your title is not already in sentence case, please mark it accordingly. **This proof page is for validation of abstract information only, and the abstract below does not necessarily appear as it will in print.** Please do not email your corrections; return your corrections via fax only no later than **Monday, December 10, 2001**. If we do not receive a return fax from you by **Monday, December 10, 2001**, your original submission will be published if accepted. **If no corrections are required, please do not fax back this proof.** We regret that our production schedule will not permit us to confirm corrections. If you have difficulty receiving attachments to email messages, please call Customer Service at (800) 375-2586 (US) or (617) 621-1398 (international). Please note that **authors' departments are not published** in the *Proceedings of the AACR* and will be deleted from the final abstract version.

**Daniel Eugene Callahan, PhD (Refer to this abstract as # 106867)**  
**Lawrence Berkeley National Laboratory**  
**1 Cyclotron Road**  
**MS 74-157**  
**Berkeley, CA 94720**  
**USA**

**A VSOM calcein assay for quantitation of multidrug resistance in human breast cancer cells**

Daniel E Callahan, Bahram Parvin, Lawrence Berkeley National Laboratory, Berkeley, CA.

In these studies we monitor the physiological responses of living cells to a series of multidrug resistance (MDR) reversal agents. The uptake and efflux of the fluorescent probe calcein (CAL) is monitored in hundreds of individual living cells. Uptake and efflux rates are obtained both in the presence and absence of various MDR reversal agents. We have assembled and tested a Visual Servoing Optical Microscope (VSOM) for these studies. VSOM studies are performed using an automated digital imaging fluorescence microscope and multiple computer-controlled perfusion pumps. With this instrument, we have quantified the loss of the MDR phenotype as a function of time spent in a drug-free tissue culture environment. A model cell system consisting of MCF-7 ADR (drug resistant, MDR) and MCF-7 WTC (drug sensitive, DS) human breast cancer cells was used. Both cell lines were cultured in DMEM with 10% FBS at 5% CO<sub>2</sub>, 37° C. We passaged DS and MDR cells 27 and 23 times, respectively, over a 24 week period. This is sufficient time for the reversion of MCF-7 ADR cells to a DS phenotype (1). For both low passage number (PN) and high PN cells, VSOM "physiological fingerprints" (calcein mean fluorescence intensity response curves) were obtained as calcein-AM (CAM) solutions were perfused into a microincubation chamber at 37° C. Multichannel digital images were acquired every 1-2 min using a 10X microscope objective. Solutions were prepared in BUFF (Dulbecco's phosphate-buffered saline containing glucose and pyruvate, pH 7.45). CAM solutions (0.25 μM) in some cases contained 10 μM MK-571 (CAM\_MK), or 50 μM verapamil (CAM\_VER). Typical VSOM CAL perfusion assays consisted of the following series of 20 min perfusion intervals: BUFF, CAM, BUFF, CAM\_MK, BUFF, CAM\_VER, BUFF. At low PN, a large difference was seen in the amount of CAL retained in DS relative to MDR cells, with MDR cells accumulating little CAL. At high PN, a distinct physiological fingerprint was still observable for MDR cells relative to DS cells, even though MDR and DS cells accumulated similar peak concentrations of CAL. The VSOM perfusion series used here is analogous to an early β-test version of an MDR assay kit developed by Solvo Biotechnology (Budapest, Hungary) for use with flow cytometers. Successful clinical trials of a similar Solvo calcein MDR assay have recently been reported (2). Our results demonstrate that VSOM calcein perfusion assays offer distinct advantages over assays performed using flow cytometers or fluorescence multiwell plate readers. Refs:(1) Budworth, J., T. W. Gant, et al. (1997). *British Journal Of Cancer* 75: 1330-5. (2) Karaszi, E., K. Jakab, et al. (2001). *British Journal of Haematology* 112: 308-14. Funded by Department of Defense, DAMD17-98-1-8177 & U.S. Department of Energy DE-ACO3-76SF00098.

**PLEASE NOTE: Receipt of this abstract proof is not a confirmation of acceptance. Notifications of abstract status will be sent out in late December.**

**PLEASE NOTE: Submitting an abstract for presentation at the 2002 AACR Annual Meeting does not constitute registration for the meeting. Online registration is available through the AACR website ([www.aacr.org](http://www.aacr.org)).**

## **Bcl-2 mRNA as a Target for Antisense Imaging Agents: Digital Imaging Fluorescence Microscope Studies of F-G3139, a Fluorescently-labeled Phosphorothioate.**

Callahan, D.E., Parvin, B.<sup>1</sup>, and Taylor, S.E., Life Sciences Division and <sup>1</sup>National Energy Research Scientific Computing Center, Lawrence Berkeley National Laboratory, 1 Cyclotron Road, Berkeley, CA 94720.

We have studied the uptake, intracellular distribution, retention, and biological effects of F-G3139 in cell lines containing constitutively high (MCF-7 "WTC") and low (MCF-7 "ADR") levels of bcl-2 mRNA. F-G3139 is 5'-(FITC)-sTsCsTsCsCsCsAsGsCsGsTsGsCsGsCsCsAsT-3', where a fluorescein phosphoramidite with a hexyl linkage was used to attach FITC to the 5' end of the all-phosphorothioate G3139 oligonucleotide. G3139 is a negatively charged 18mer that targets the first six codons of the bcl-2 mRNA open reading frame. Living cells were imaged (63X oil-immersion objective, NA 1.3) for several hours in a temperature-controlled microscope perfusion chamber using both transmitted and fluorescence light. A Hamamatsu C4880 cooled CCD camera was used to acquire digital images. Washout curves generated from WTC and ADR cells loaded with F-G3139 were significantly different at 37° C, with F-G3139 washing out less readily from the high bcl-2 WTC cells. However, ADR cells have higher levels of the transmembrane multidrug transporter molecule P-glycoprotein (Pgp) than WTC cells, thus, the presence of Pgp and not the intrinsically lower levels of bcl-2 mRNA may be responsible for the lower accumulation and retention in ADR cells. In order to determine whether F-G3139 is a substrate for Pgp, we obtained uptake and washout curves for F-G3139 in the presence and absence of 25 µM verapamil, a competitive inhibitor of Pgp; preliminary results indicate that F-G3139 may be a substrate for Pgp. In a separate set of studies, living WTC and ADR cells were prestained with the membrane-permeable nuclear dye Hoechst 33342 ("H42", 1.75 µM) under serum-free conditions (DPBS containing glucose and pyruvate, pH 7.4). This fluorescent dye is often used to stain the nucleus of living cells. We found that cells exposed to H42 for several hours rounded up and underwent a membrane permeability transition characteristic of the early stages of apoptosis. This increase in membrane permeability was detected using the nuclear stains YO-PRO-1 and/or YO-PRO-3. In rounded cells that stained positive for increased membrane permeability, a large increase in the amount of F-G3139 fluorescent signal was also observed. Both WTC and ADR cells exhibited a similar increase in fluorescence intensity that was concentrated in the nucleolar regions of the nucleus. Under similar conditions, in the absence of H42, cells of both types that remained flattened and well attached displayed a distinctive F-G3139 cytoplasmic staining. In a third set of studies, apoptosis was induced in WTC and ADR cells by glucose deprivation in the presence of glucose-free fetal bovine serum. Under these conditions, exposure to 0.7 µM, 2.0 µM, and 4.0 µM F-G3139 was cytotoxic to WTC, but not ADR cells. This is consistent with previous results which have demonstrated that non-fluorescent anti-bcl-2 antisense compounds are cytotoxic to cells with constitutively high levels of bcl-2.

*Funded through the Office of Biological and Energy Research, Molecular Nuclear Medicine Program in the Office of Science, U.S. Department of Energy, under contract DE-ACO3-76SF00098.*



• **Appendix E: Poster & Abstract, 2001 Biophysical Society Annual Meeting**



# 1 ABSTRACT

Callahan, D.E. and Parvin, B., *Biophysical Journal* **80**, 169a.

## VISUAL SERVOING FOR THE DETECTION, QUANTITATION, AND MODULATION OF SPECIFIC CELL RESPONSES IN SUBPOPULATIONS OF MULTIDRUG RESISTANT (MDR) HUMAN BREAST CANCER CELLS.

Callahan, D.E.<sup>1</sup>, and Parvin, B.<sup>2</sup>, <sup>1</sup>*Cell and Molecular Biology Department, Life Sciences Division,* <sup>2</sup>*High Performance Computing Research Department, National Energy Research Scientific Computing Center (NERSC), High Performance Computing Research Department, Lawrence Berkeley Laboratory, 1 Cyclotron Road, Berkeley, CA 94720*

MDR can be dependent on transmembrane proteins (e.g., PgP and MRP) that extrude foreign compounds. Expression of these proteins is indicated by reduced accumulation of calcein. An automated digital imaging fluorescence microscope was used to perfuse calcein-AM (CAM, 0.25 $\mu$ M) containing modulating agents MK-571 (10 $\mu$ M) or verapamil (50 $\mu$ M) into a microperfusion cell chamber. MK-571 is a specific inhibitor of MRP, while verapamil inhibits both PgP and MRP. MCF-7ADR cells labeled with Hoechst 33342 were observed at 35°C. Mean fluorescence intensity per cell (MI, calcein) was calculated in real-time and software operation of syringe pumps was based on these calculations; hence, the term *visual servoing*. The protocol found in an MDR Beta-Test Kit (Molecular Probes, Eugene, OR), was modified. Images were acquired during perfusion intervals **(1)** 0-2100s, CAM, **(2)** 8600-11000s, CAM+MK-571, and **(3)** 14000-16000s, CAM+verapamil. All cells responded by **3**. Subpopulations expressing MRP and/or PgP can be inferred based on responses where  $\Delta MI > 200$  ( **FIGURE 1**): (a) Responses in **1** (no PgP or MK-571) (b) None until **2** (MRP) (c) None in **1** or **2** (PgP only) *Funded by Department of Defense, DAMD17-98-1-8177 & U.S. Department of Energy DE-ACO3-76SF00098.*

# 1 (ABSTRACT, cont.)

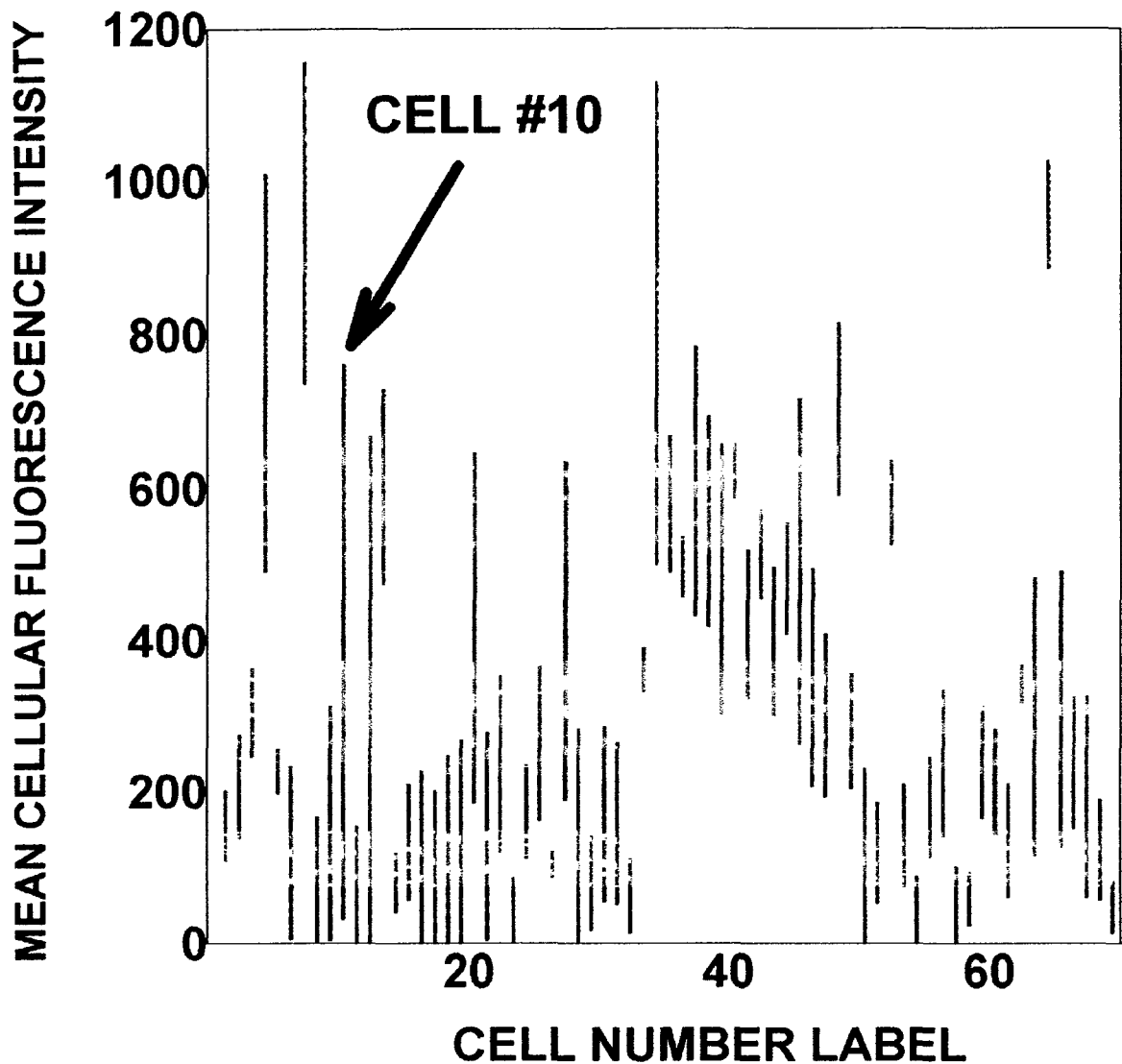


**FIGURE 1: CAM+MK-571 perfusion, interval 2 (8600 - 11000s).**

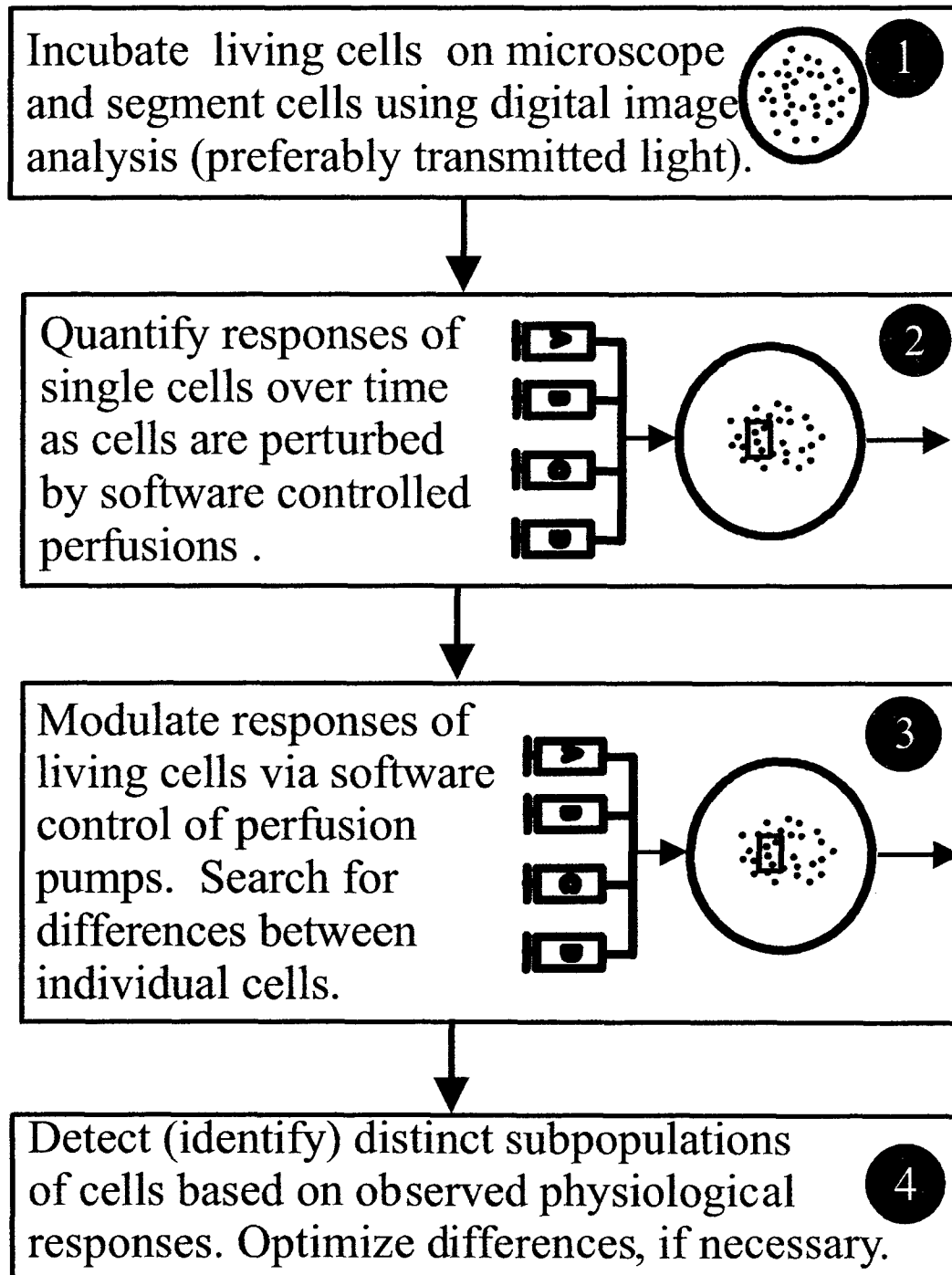
The 2D projection of MI versus time for 69 cells is shown.

Time axis is perpendicular to the plane of the page. The increase in MI due to calcein accumulation was greater than 200 in 30 cells, due to inhibition of MRP by MK-571. Three digital images (channels) were acquired every 60s. The MI of cell #10, for example, increased from 30 to 760 (arrow) during this 2400s perfusion interval.

# 2



## Visual Servoing Optical Microscopy (VSOM) for the Detection of Cell Subpopulations



## 2 (cont)

### METHODS & MATERIALS

**CELL LINES:** A well characterized pair of drug-sensitive (DS) and multidrug resistant (MDR) cell lines were used in these studies. Both the DS cell line (MCF-7 WTC) and the MDR cell line (MCF-7 ADR) were obtained from Dr. Amadeo Parissenti (North Eastern Ontario Regional Cancer Centre (NEORCC), Sudbury, ONT, Canada). Dr. Parissenti obtained his cell lines directly from the published originator (Dr. Kenneth Cowan).

**â-test kit for a MultiDrug Resistance (MDR) Assay :** Both our lab and Dr. Parissenti tested these cell lines using a kit a being developed by Molecular Probes (Eugene, OR; Contact Vicki Singer, Ph.D. at 541-465-8300 x306 or VickiSinger@probes.com). The â-test kit is being developed for use with flow cytometers. Dr. Parissenti has verified differential calcein accumulation via two distinct MDR mechanisms in these cell lines using the â-test kit and flow cytometric methods. Dr. Parissenti has also performed other characterizations of these cell lines. This provided us with an opportunity to compare VSOM results with flow cytometric results.

**Principles of the kit:** The acetoxymethyl ester (AM) derivative of the intensely fluorescent dye, calcein (CAM), is a relatively nonfluorescent, nonpolar, lipophilic molecule that can normally diffuse passively across the plasma membrane. Once inside the cell, the AM group is cleaved from CAM by intracellular esterases. The resulting molecule, calcein, is negatively charged, hydrophilic, and is normally retained within the cell. However, most cells have the ability to produce on demand (overexpress), a variety of transmembrane proteins that are energy (ATP) -dependent transporters, or pumps. Once one or more of these proteins is overexpressed, the cell is said to have acquired the multidrug resistance (MDR) phenotype. Interestingly, any given MDR protein has a broad spectrum of substrates (including many anticancer drugs and fluorescent dyes) that can be actively extruded, thus protecting the cell from possible cytotoxic effects. Depending on the MDR molecule, the substrate may be intercepted while passing through the plasma membrane, or the substrate may be internalized before it is pumped out. Substrates that can be extruded by a given MDR protein need not be related structurally, or functionally. The model cell system we have chosen for these MDR studies is the MCF-7 Wild Type Cowan (MCF-7 WTC) and the MCF -7 adriamycin (doxorubicin) -resistant line MCF-7 ADR. MCF-7 ADR cells are known to express both the 170 kDa P-glycoprotein (PgP) and the 190 kDa Multidrug Resistance Protein (MRP). However, MCF-7 WTC cells express MRP only. Separate genes code for these two different proteins. The drug cross-resistance profiles, or spectra, of these two proteins overlap, but are not identical. In addition, these two different proteins have different sensitivities to various inhibitors, and this is the basis of the assay studied here.

Additional experimental details are provided throughout this poster in the Figure Legends.

3

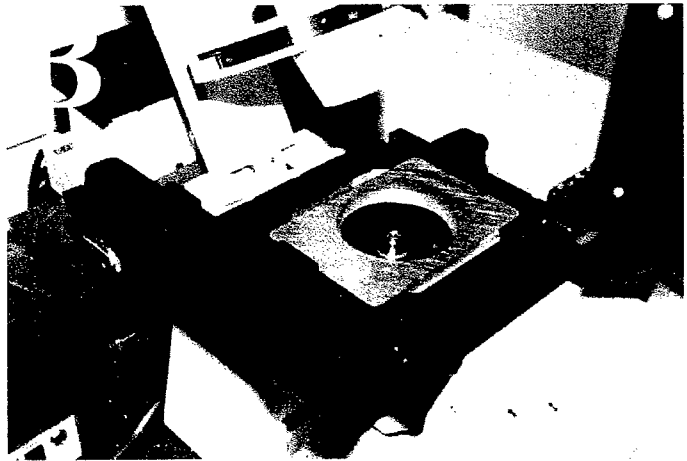
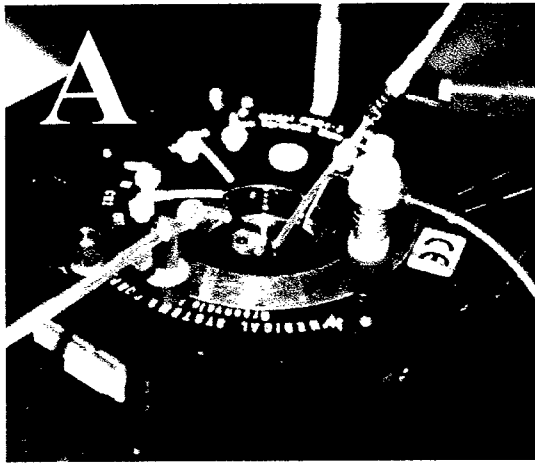
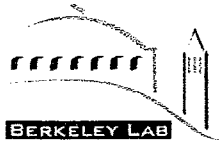


**FIGURE 3: PHOTOS (A)** A temperature-controlled microperfusion chamber (PDMI-2, Harvard Apparatus) was mounted on a Zeiss Axiovert microscope **(B)**. A bipolar temperature controller (TC-202) was used with the PDMI-2. This is a Peltier electronic instrument that delivers and adjusts DC current to the microincubator to control temperature. A "Bath" type thermistor (BSC-T3, 36K Ohms total) was used with the PDMI-2. The Zeiss Axiovert 135 H/DIC, TV inverted microscope was used for transmitted light (phase and DIC) and multicolor fluorescence microscopy. It is equipped with a computer controlled xy scanning stage, z-axis stepping motor, and six position filter wheel. A 12-bit Xillix CCD camera (Xillix Technologies, Vancouver, BC) containing a Kodak KAF-1400 CCD chip (1317x1035 pixels, 7x7 micron pixel size) was used for these studies. This camera has a readout rate of 8 MHz (approximately four full size images per sec). Images from the cameras are readout directly into a Sparcstation Ultra 1, a multitasking UNIX workstation that can store or transfer images across the network during the course of the experiment. A 100 BaseT network line linked the computers and microscope to the computers of the Imaging Technology and Distributed Computing Group. This inverted microscope has a base port so that cameras mounted below obtain better fluorescence signal. In addition, the inverted design allows perfusion of living cells, with cells located on the bottom of a microperfusion cell chamber. With this design it is possible to switch from fluorescence to transmitted light detection (phase or DIC) and verify cell locations, morphology, etc. This is achieved with a computer controlled transmitted light shutter. A computer controlled epifluorescence shutter is also available in the filter wheel. Two computer controlled, dual syringe pumps (Harvard 33, Harvard Apparatus) were used. Each syringe has its own, computer controlled block so that perfusion rates can be controlled independently.

# 3 (cont.)

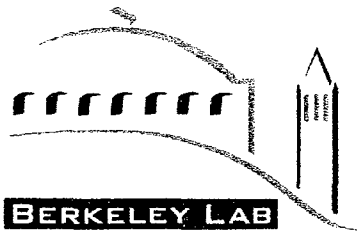
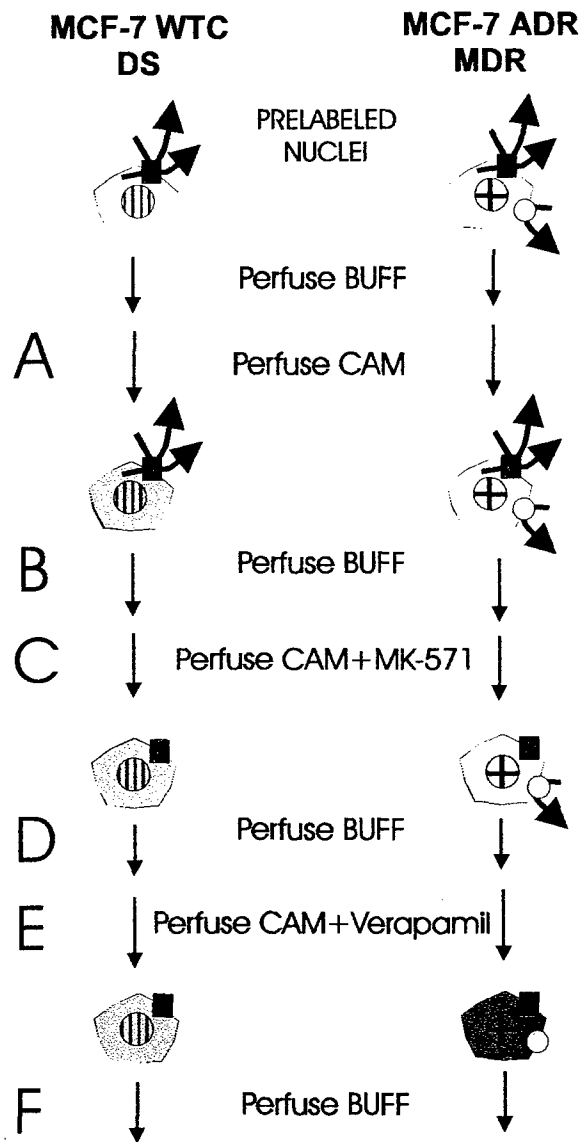


**FIGURE 3: SCHEMATIC OF MDR ASSAY:** As seen in this schematic, MCF-7 WTC and MCF-7 ADR cells accumulate and retain internal calcein (GREEN) at rates that are dependent upon the presence of MDR proteins in the cytoplasmic membrane. MCF-7 ADR cells are able to pump out calcein, unless one or more inhibitors of PgP and MRP are present. In this schematic arrows indicate active pumps. Pumps that have been inhibited by MK-571 or Verapamil are inactive as indicated by the absence of pump arrows. Compare this schematic to the pump interval schematic in Figure 4 (A).



- **MRP:** Pumps Calcein out of Cytosol, and pumps Calcein-AM out of plasma membrane. It is inhibited by both MK-571 and Verapamil.
- **PgP:** Pumps Calcein-AM out of plasma membrane, and is inhibited by Verapamil

# 4

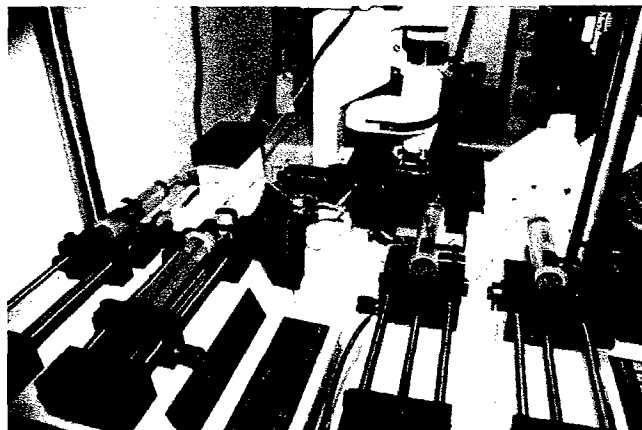


**FIGURE 4: PHOTO** Two Computer controlled, dual syringe pumps (Harvard 33, Harvard Apparatus) are shown. Four independently controlled syringes were used in these experiments. However, up to 99 pumps can be daisy-chained together.

**FIGURE 4: SCHEMATIC OF PERFUSION INTERVALS:** (A) The composition each syringe solution is indicated. In addition, the time and magnitude (perfusion rate in mL/min) of each perfusion pulse is indicated (a-g). This an example of an experiment using continuous perfusion intervals. Compare these perfusion intervals (a-g) with the steps (a-g) shown in the Figure 3 schematic. (B) Results for MCF-7 WTC cells. A screen snapshot of the mean responses of all cells in the field. This graph is displayed in real time during the VSOM experiment. It has been scaled so that it matches the time scale in (A). (C) Results for MCF-7 ADR cells. Screen snapshot of the mean responses of all cells in the field of view.

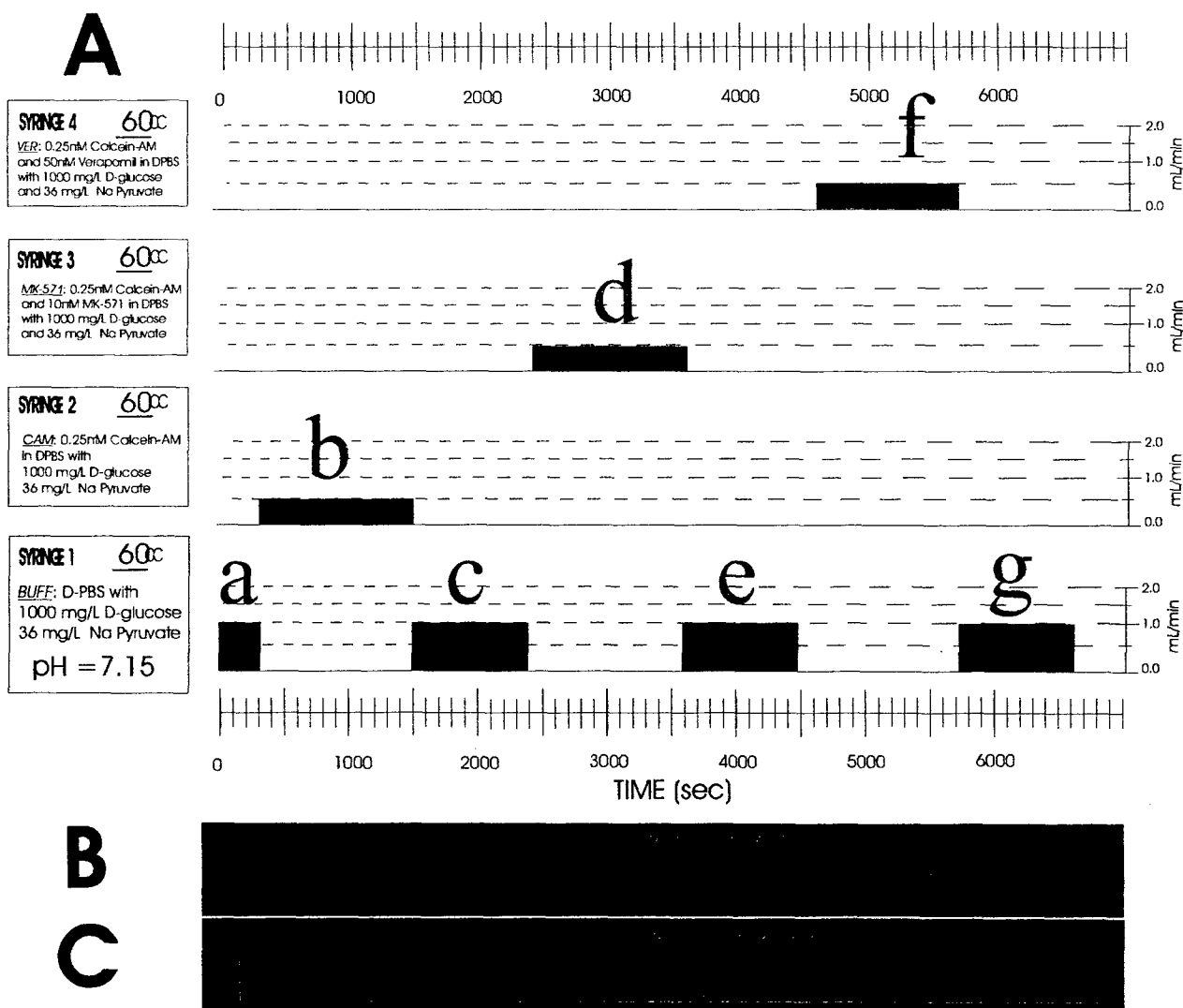
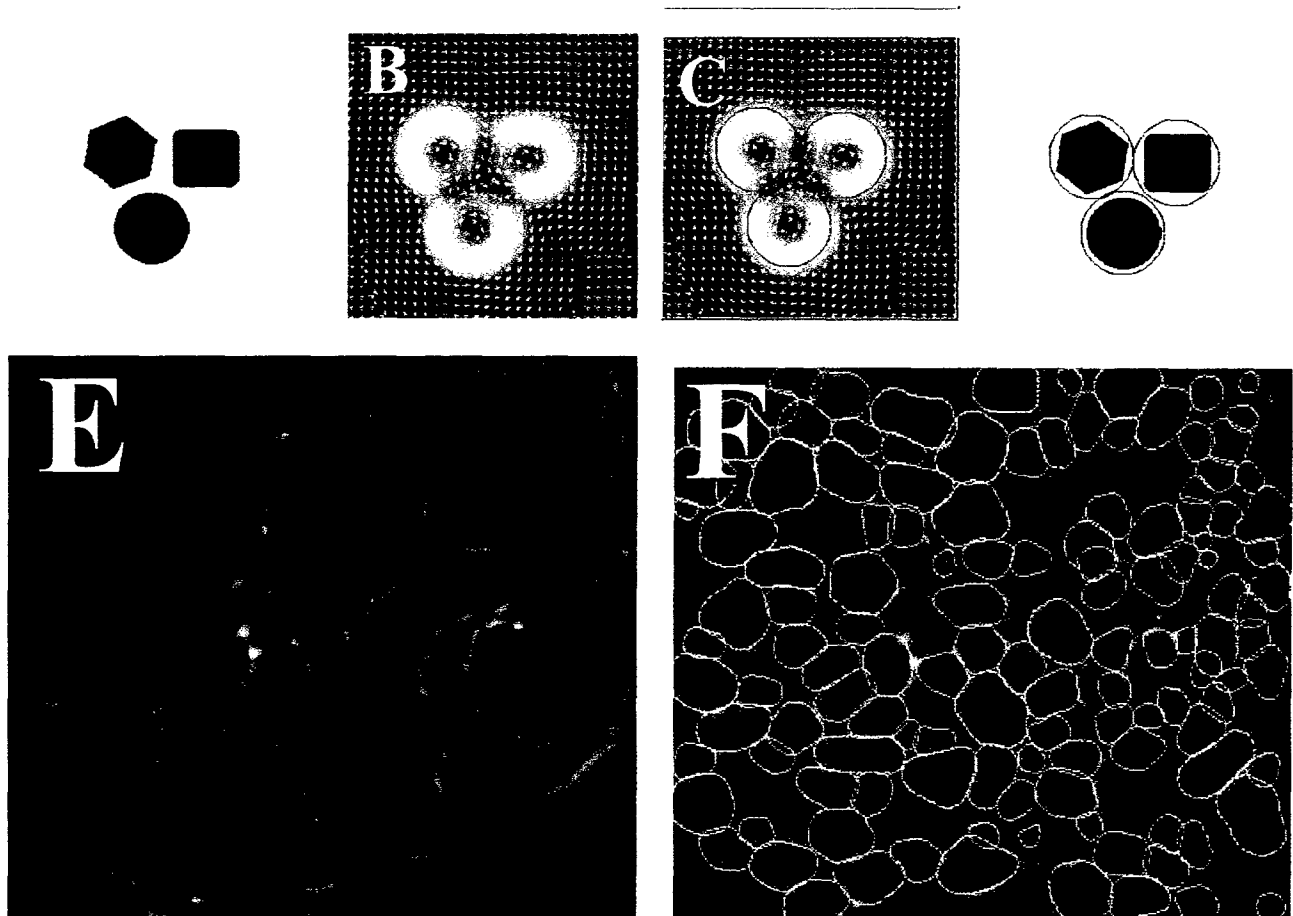


**FIGURE 5: DIGITAL IMAGE SEGMENTATION TECHNIQUES**

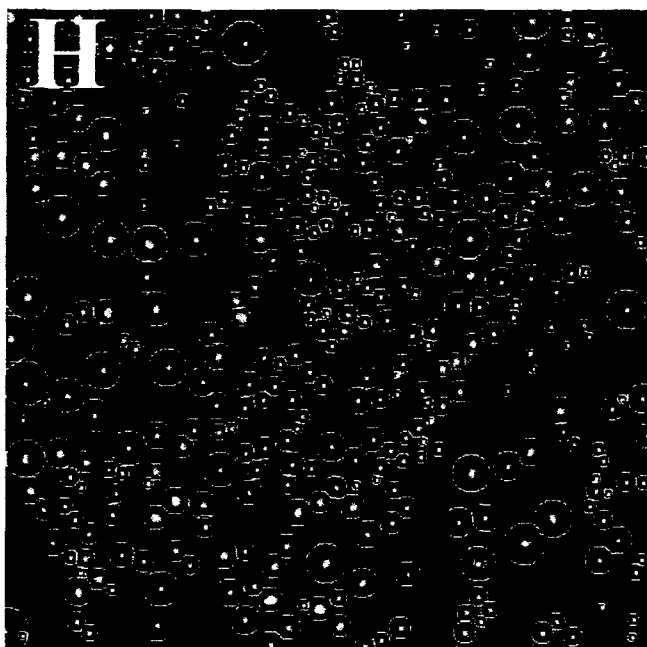
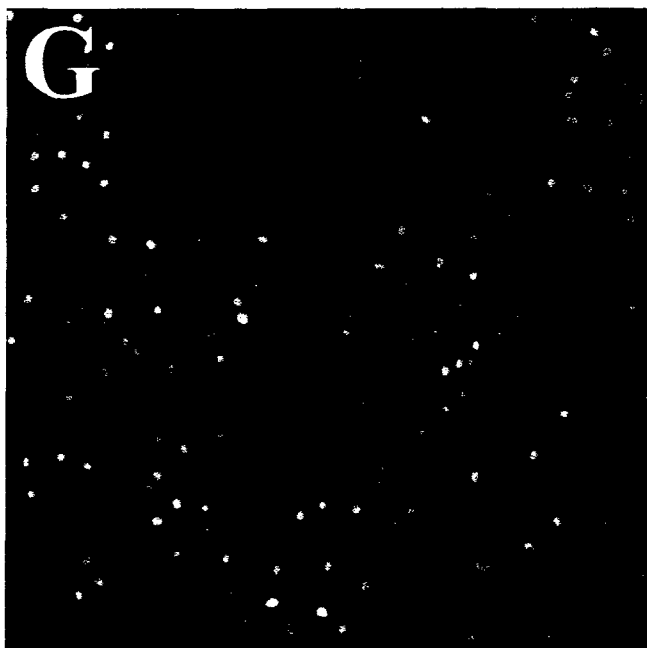
Recently, we have developed several new techniques. One is based on a vector representation of the underlying image followed by feature extraction in vector space, and another is based on a geometric and texture model of a cell and its interaction with neighboring cells.

**Figures 5A-D** The vector representation technique has its root in analysis of spatio-temporal satellite images. These images show intermediate and final results of this segmentation technique (on a synthetic image).

**Figures 5E,F** show vector representation results on living cells imaged using a 20X phase contrast object and transmitted light. One of our goals is the development of segmentation techniques that work equally well with transmitted light and fluorescence digital images.



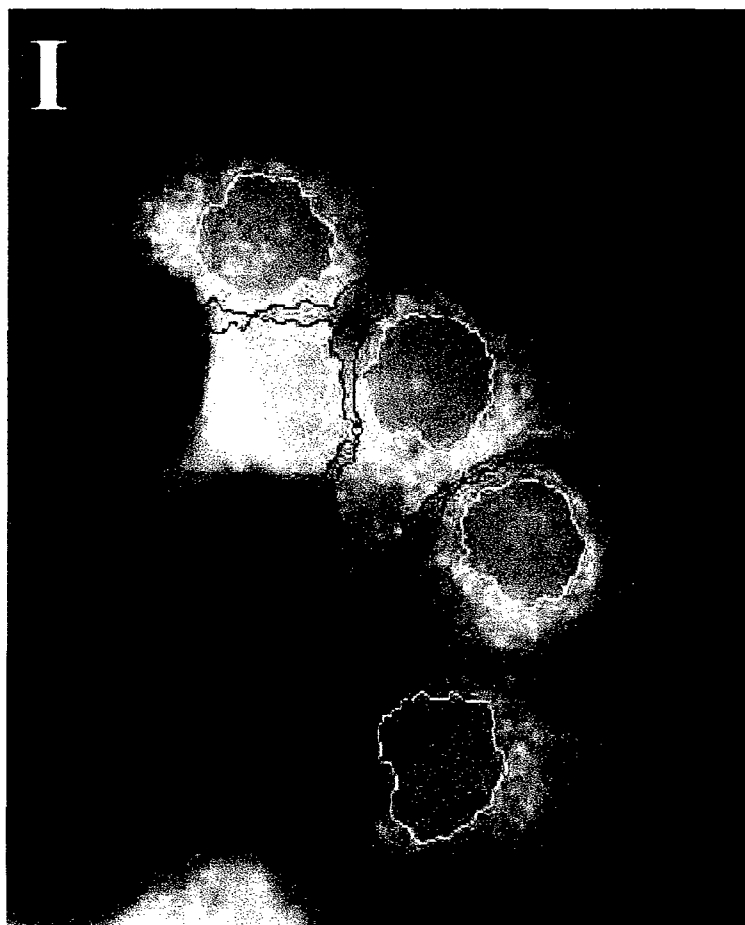
# 5B (cont.)



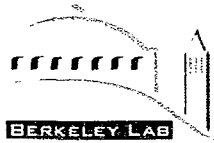
Figures 5G,H shows an intermediate step in a vector representation computation. This image was acquired using a 10X Fluar objective and shows the nuclei of living and lysed cells that have been labeled with the fluorescent dye Hoechst 33342.

Figure 5I is a demonstration of the Geometric and texture model technique. Although the previous techniques are applicable for localizing nuclei, a more advanced technique is needed for a more detailed segmentation at higher imaging resolutions. This is based on a geometric model of the cell, its texture in various compartments, and the relationship of its features with respect to one another. The geometric model is expressed as a graph, and the texture is computed using an array of orientation and scale specific filters. These local feature activities help collect an ensemble of information that is further refined with dynamic programming. In this image, MCF-7 cells have been stained with TMRE, a mitochondrial and cytoplasm stain useful for monitoring the membrane potential of the mitochondrial and plasm membrane.

NOTE: Figure 5I was acquired using a 63X, oil immersion objective. Figures 5E,F were acquired using a 20X objective. All other images were acquired using a 10X, NA 0.5 Zeiss Fluar Objective. In all cases, digital images were 1024x1024. The CCD chip in our camera has pixels of the size 6.8x6.8  $\mu$ m. Thus, all images taken at 10X show a field of view that is approximately 700 $\mu$ m high and 700 $\mu$ m wide.

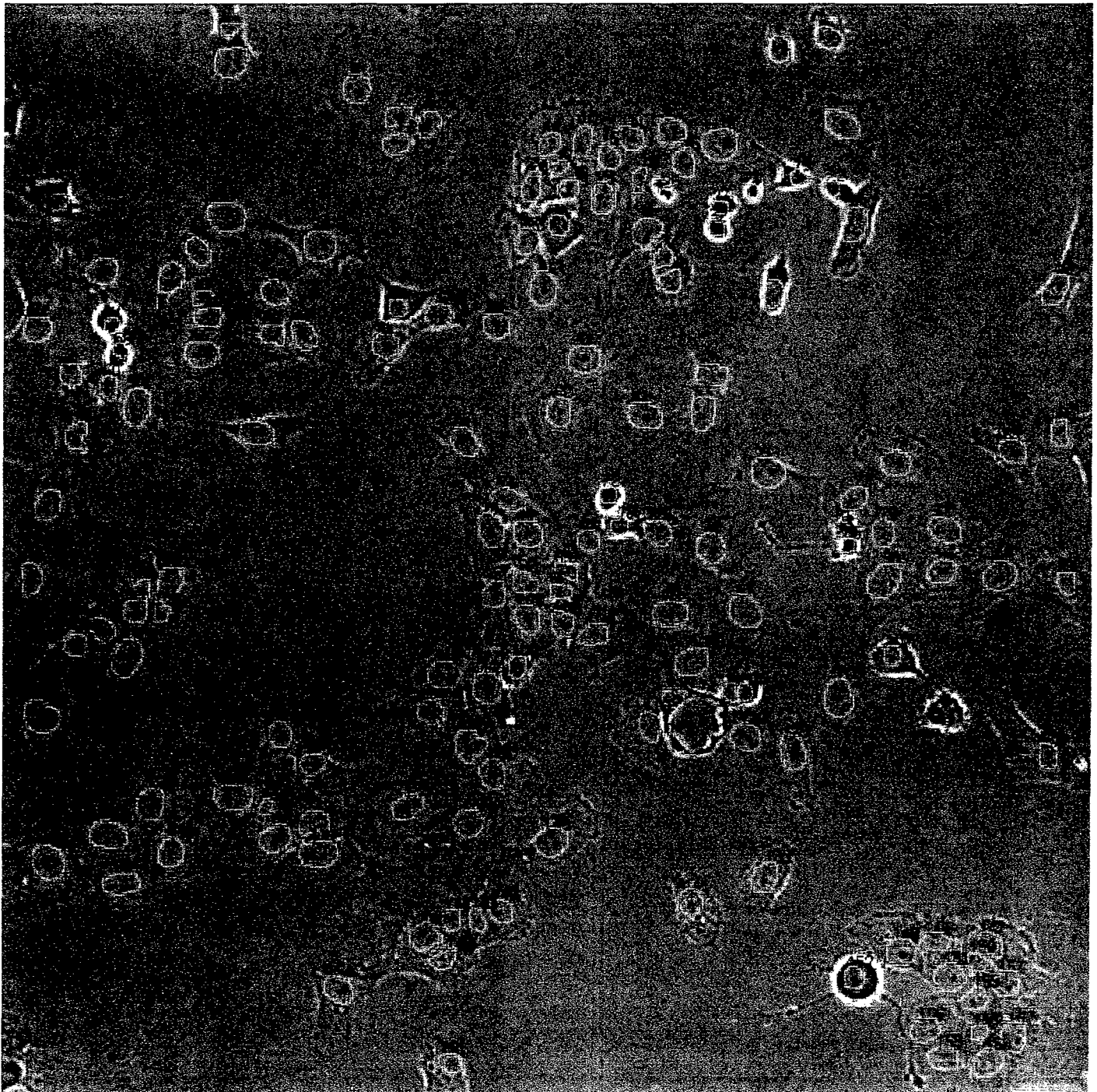


# 6A



## **FIGURE 6: EXAMPLE OF CURRENT SEGMENTATION RESULTS**

(A) Nuclei of living cells were prestained with Hoechst 33342 (H42) as shown in Figure 3 schematic. Digital images of the cells were then acquired in three separate channels: transmitted light, 360nm excitation (blue fluorescence), and 490nm excitation (green fluorescence). Cell nuclei were segmented using the blue channel image. The resulting contours are shown here, overlaid on the transmitted light channel (time zero image).

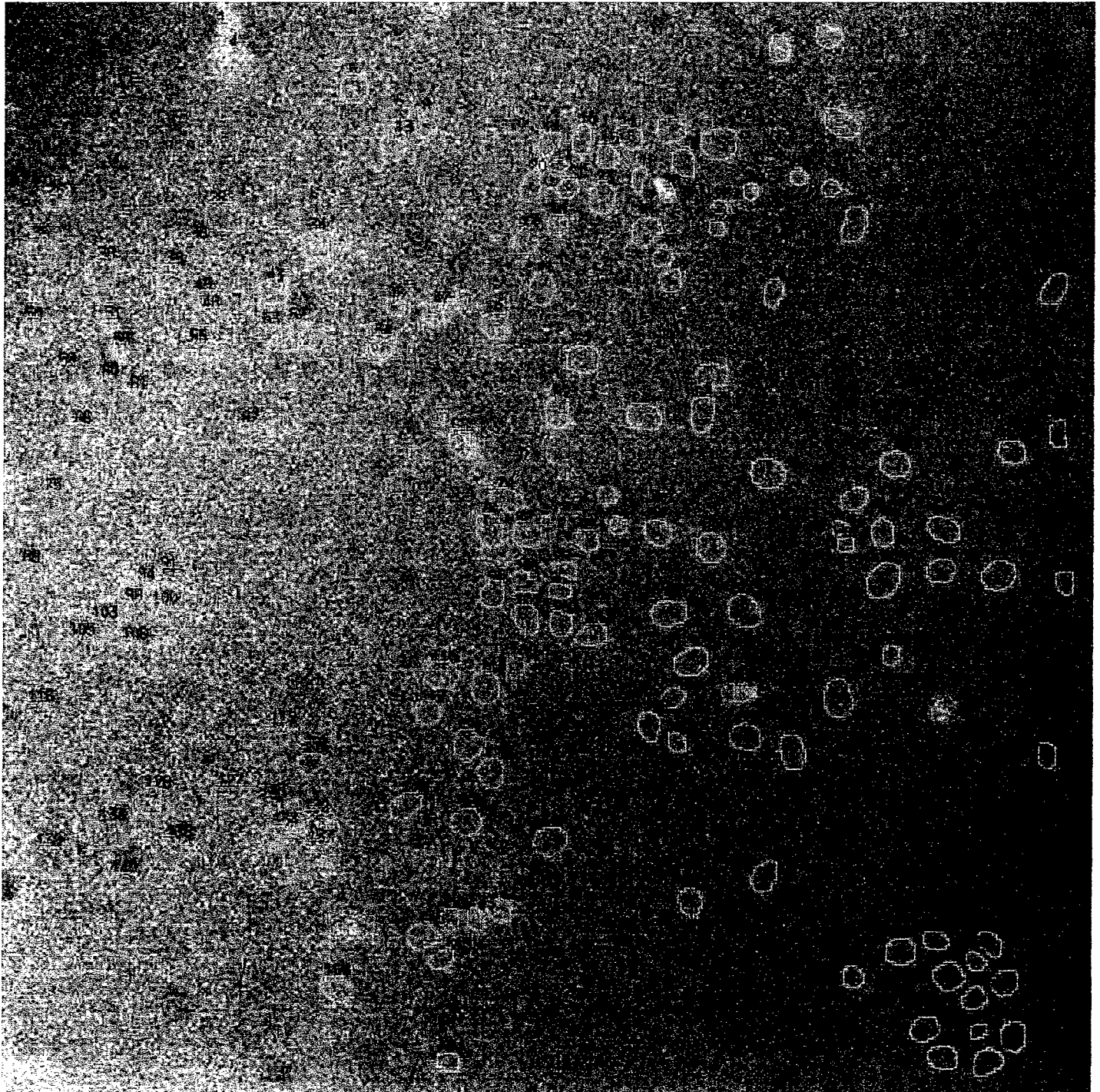


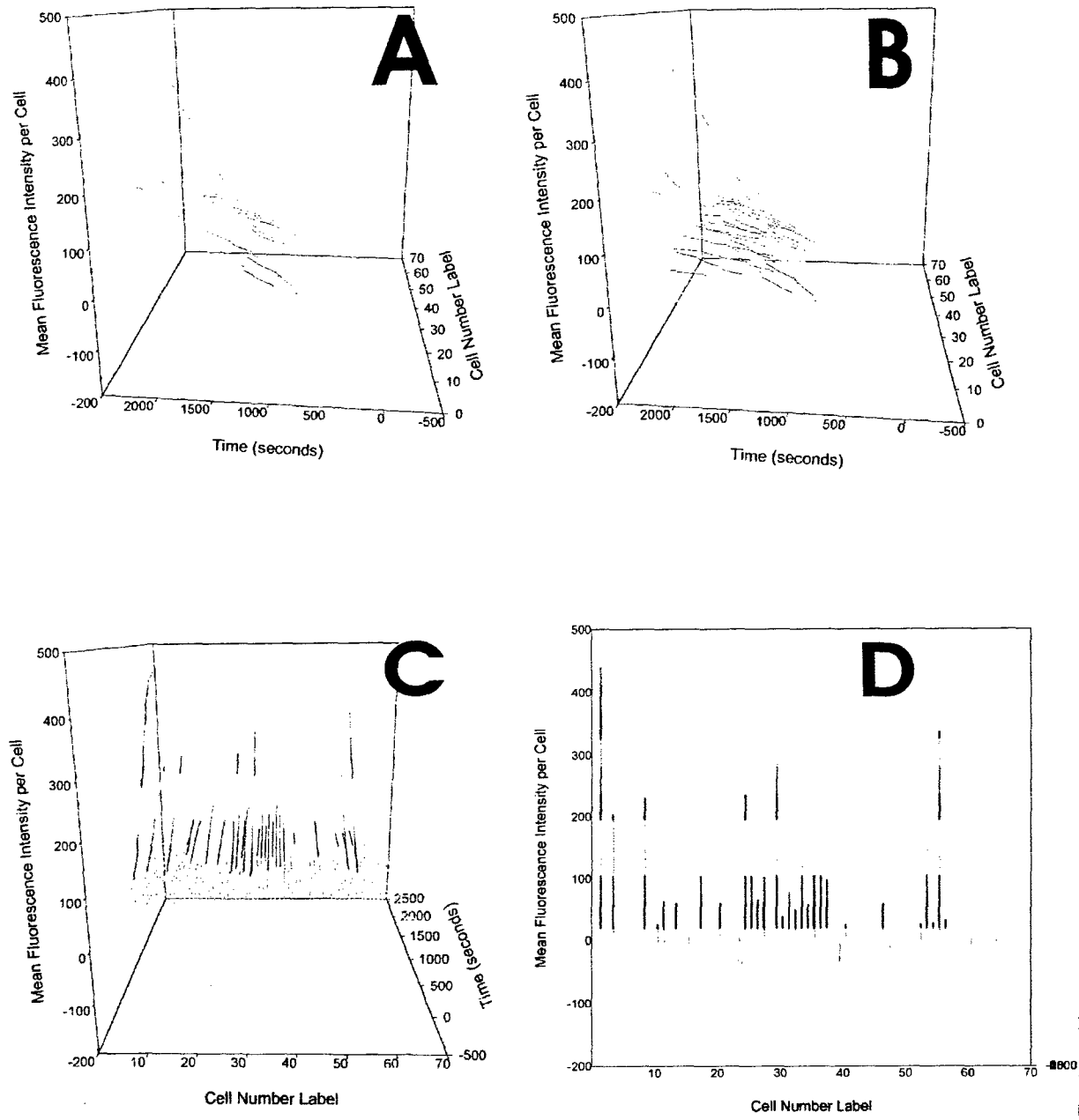
# 6B



## **FIGURE 6 (cont.): EXAMPLE OF CURRENT SEGMENTATION RESULTS**

**(B)** The green channel image at time zero with overlaid contours (same contours as in A). At this point, there is zero calcein accumulation and very little background fluorescence from the blue channel or from cellular autofluorescence.





**Discontinuous Perfusion Intervals: Cell responses from perfusion interval (1) (Compare to perfusion interval (2) in FIG 1 of ABS TR ACT). Calcien accumulation in 65 MCF-7 ADR cells during Calcien-AM perfusion. Cells that accumulate calcien are not multi-drug resistant. Four views of the same data are shown. (A) Selected responses of 14 cells that accumulated calcien. 3D response curves are color coded according to intensity (B) All 65 cell responses shown. Many MDR cells are evident. (C) All 65 cell responses viewed end-on (D) 2D projection of the 3D data shown in C.**



**FIGURE 8: CONTINUOUS PERFUSION INTERVALS**

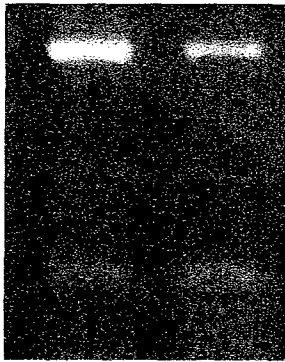
The perfusion schedule shown in Figure 4A (pulses a-g) was applied to MCF-7 WTC cells (Figure 8E) and to MCF-7 ADR cells (Figure 8F). The individual cell responses are shown as a function of time. As seen in Figure 8G, MCF-7 WTC cells have more MRP protein than do MCF-7 ADR cells. However, MCF-7 ADR cells have much more PgP protein than do MCF-7 WTC cells (Figure 8H).

Evidence of the MRP protein is seen in the ability of MCF-7 WTC cells to extrude intracellular calcein during perfusion interval c (a wash-out step). However, the absence of PgP is clearly indicated by the lack of a calcein uptake in the presence of verapamil (interval f). As seen in Figure 8F, the majority of MCF-7 ADR, with high levels of PgP, shown a response during interval f.

Thus, VSOM results are consistent with the known phenotypes of these cell lines.

**G**

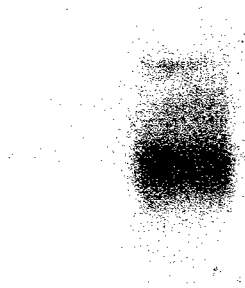
MRP mRNA levels



WT    ADR

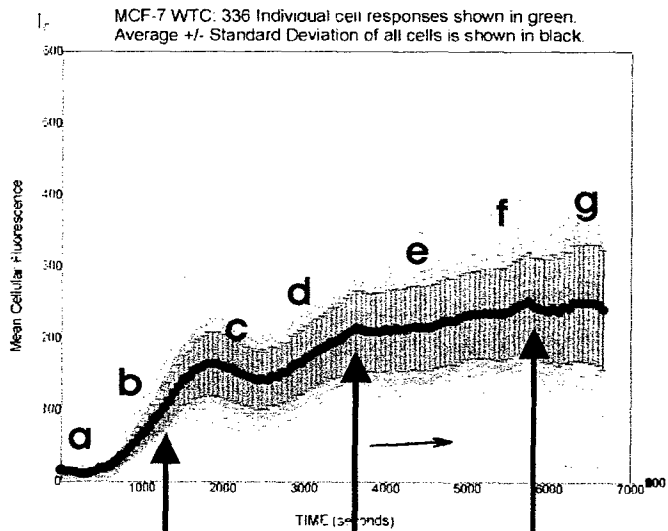
**H**

Pgp protein levels

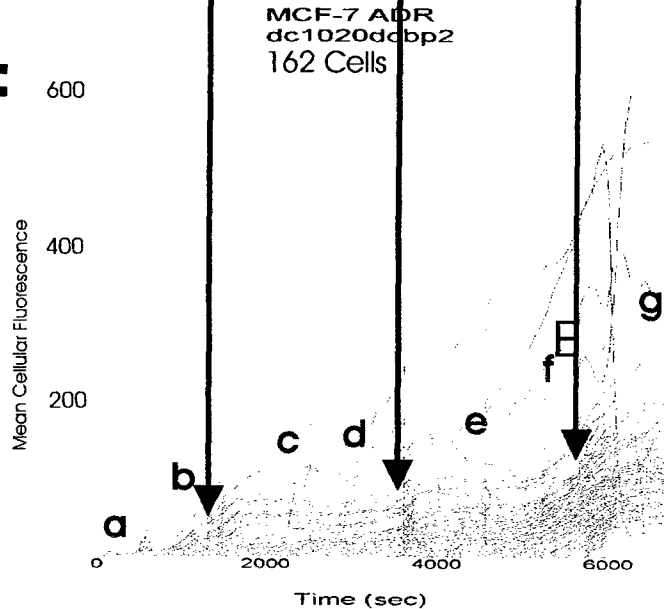


WT    ADR

**E**



**F**





## Conclusions:

- We have adapted an MDR test kit designed for flow cytometry to our VSOM system. Several advantages exist in VSOM assays relative to flow cytometric assays. For example, individual cells can be repeatedly stimulated and these perturbations can be adjusted in real-time based on the on-going analysis of dynamic, single-cell physiological responses.
- VSOM results were seen to be consistent with the known phenotypes of these cell lines, and with flow cytometry results obtained by our collaborator, Dr. A. Parissenti.
- Several distinct subpopulations of MDR cells exist in the MCF-7 ADR cell line, and were identified on the basis of distinct physiological responses.
- These preliminary results indicate that a single MDR cell in an entire field of cells could easily be detected (1 in 1000 cells).



## Acknowledgements:

Research funded by the Department of Defense, Breast Cancer Research Program, under the U.S. Army Medical Research and Materiel Command, contract number DAMD17-98-1-8177.

Also by U.S. Department of Energy DE-ACO3-76SF00098.

• **Appendix F: LBNL Software Disclosure Form (for VSOM1 Software)**

• **Appendix G: Grant Proposal to NSF/NIGSM**

•  
\* **Appendix H: Grant Proposal to CA BCRP Cycle 7 (not funded)**

• **Appendix I: Patent Disclosure IB-1559 P1 for VSOM Control Software**

## **Appendix J: Publications Resulting from this Research**

1. Callahan, D.E., and Parvin, B. **Quantitation of Single Cell Responses using Fluorescence Microscopy**, *Proceedings: Era of Hope Department of Defense Breast Cancer Research Program Meeting, Volume 2, page 709*. Atlanta, GA, June 8-11, 2000, Poster Number: CC-5.
2. Callahan, D.E., and Parvin, B. **Visual Servoing for the Detection, Quantitation, and Modulation of Specific Cell Responses in Subpopulations of Multidrug Resistant (MDR) Human Breast Cancer Cells**, Biophysical Society Annual Meeting 2001, Boston, MA, February 17-21, 2001, Abstract Number: 3275.
3. Callahan, D.E., and Parvin, B. **A VSOM calcein assay for quantitation of multidrug resistance in human breast cancer cells**. *To be presented at "A VSOM calcein assay for quantitation of multidrug resistance in human breast cancer cells"*, to be presented at the 93rd Annual Meeting of the AACR, San Francisco, April 6-10, 2002, *ABSTRACT ID 10686*.
4. Callahan, D.E., and Parvin, B. **BioSig: A Database for Efficient VSOM Extraction of Dynamic Phenotypic Data from Individual Living Cells** *to be presented in a Platform Session* (Session Title: Platform S - Biophysical Chemistry & Emerging Techniques, Monday, February 25, 2002) at the Biophysical Society Annual Meeting in San Francisco, California, February 23-27, 2002 (Program #860-Plat).

**Appendix K: Personnel receiving pay from this research**

1. Callahan, D.E.

2. Parvin, B.

**Appendix L: ABBREVIATIONS & ACRONYMS:**

<b>AML</b>	acute myeloid leukemia
<b>AROP</b>	the approved revisions to the original proposal (July 1998)
<b>AR#1</b>	the Year 1 Annual Report (October 1999)
<b>AR#2</b>	the Year 2 Annual Report October 2000)
<b>CR</b>	complete remission
<b>DOE</b>	U.S. Department of Energy
<b>G3139</b>	anti-Bcl-2 antisense compound
<b>JCFG</b>	Our Java Command File Generator software
<b>MDR</b>	multidrug resistance/resistant
<b>MK-571:</b>	(3-({3-(2-[7-chloro-2-quinoliny]ethenyl)phenyl}-(3-dimethylamino-3-oxopropyl)thio)methyl]thio)propanoic acid)
<b>MRP:</b>	multidrug resistance-associated protein, product of the <i>MRP</i> gene
<b>MS:</b>	Microsoft
<b>Pgp:</b>	P-glycoprotein, product of the <i>MDR1</i> gene
<b>OBER</b>	Office of Biological and Environmental Research in the Office of Science of DOE
<b>OP</b>	the original proposal (June 1997)
<b>VSOM</b>	Visual Servoing Optical Microscope/Microscopy



DEPARTMENT OF THE ARMY  
US ARMY MEDICAL RESEARCH AND MATERIEL COMMAND  
504 SCOTT STREET  
FORT DETRICK, MARYLAND 21702-5012

REPLY TO  
ATTENTION OF:

MCMR-RMI-S (70-1y)

21 Feb 03

MEMORANDUM FOR Administrator, Defense Technical Information  
Center (DTIC-OCA), 8725 John J. Kingman Road, Fort Belvoir,  
VA 22060-6218

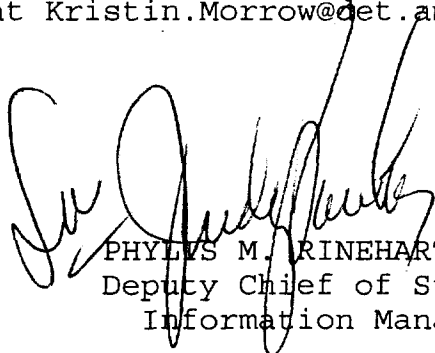
SUBJECT: Request Change in Distribution Statement

1. The U.S. Army Medical Research and Materiel Command has reexamined the need for the limitation assigned to technical reports written for this Command. Request the limited distribution statement for the enclosed accession numbers be changed to "Approved for public release; distribution unlimited." These reports should be released to the National Technical Information Service.

2. Point of contact for this request is Ms. Kristin Morrow at DSN 343-7327 or by e-mail at Kristin.Morrow@det.amedd.army.mil.

FOR THE COMMANDER:

Encl

  
PHYLLIS M. RINEHART  
Deputy Chief of Staff for  
Information Management

ADB263458	ADB282838
ADB282174	ADB233092
ADB270704	ADB263929
ADB282196	ADB282182
ADB264903	ADB257136
ADB268484	ADB282227
ADB282253	ADB282177
ADB282115	ADB263548
ADB263413	ADB246535
ADB269109	ADB282826
ADB282106	ADB282127
ADB262514	ADB271165
ADB282264	ADB282112
ADB256789	ADB255775
ADB251569	ADB265599
ADB258878	ADB282098
ADB282275	ADB232738
ADB270822	ADB243196
ADB282207	ADB257445
ADB257105	ADB267547
ADB281673	ADB277556
ADB254429	ADB239320
ADB282110	ADB253648
ADB262549	ADB282171
ADB268358	ADB233883
ADB257359	ADB257696
ADB265810	ADB232089
ADB282111	ADB240398
ADB273020	ADB261087
ADB282185	ADB249593
ADB266340	ADB264542
ADB262490	ADB282216
ADB266385	ADB261617
ADB282181	ADB269116
ADB262451	
ADB266306	
ADB260298	
ADB269253	
ADB282119	
ADB261755	
ADB257398	
ADB267683	
ADB282231	
ADB234475	
ADB247704	
ADB258112	
ADB267627	